MINISTRY OF SUPPLY

AERONAUTICAL RESEARCH COUNCIL
REPORTS AND MEMORANDA

Wind-Tunnel Measurements of Yawing Moment due to Yawing (n_r) on a $1/5 \cdot 5$ Scale Model of the Meteor Mark F.III

By

J. G. Ross, B.Sc.(Eng.), D.I.C., A.M.I.Mech.E., A.F.R.Ae.S.
and
R. C. Lock, M.A.

LONDON: HER MAJESTY'S STATIONERY OFFICE

1952

PRICE 8s. 6d. NET

Wind-Tunnel Measurements of Yawing Moment due to Yawing (n_r) on a 1/5.5 Scale Model of the Meteor Mark F.III

By

J. G. Ross, B.Sc.(Eng.), D.I.C., A.M.I.Mech.E., A.F.R.Ae.S.

and

R. C. Lock, M.A.

Summary.—During recent investigations into the self-excited oscillations in yaw, experienced on *Meteor* aircraft, the lateral stability derivative, n_r, was measured in flight, and found to differ considerably during initial experiments from the theoretical estimate.

A new technique was therefore devised to measure n_r in the wind-tunnel; and, with its aid, modifications were tested on a model with the object of reducing the self-excited oscillations in flight. Measurements of n_r were made over a range of Reynolds numbers, and for different periods of oscillation of the model.

The final comparison of the flight and wind-tunnel tests, after certain refinements in technique of the former, and after corrections for solid friction to the latter had been made, showed that the full-scale measurement of n_r was about 10 per cent less than that obtained in the tunnel. Considering the difficulties involved, this agreement may be considered as satisfactory.

For the model in the standard condition, the value of n_r was about 20 per cent less than the estimated figure of —0·108 at zero lift, but with dorsal fins (*see* sections 5.7 and 5.8). It was found possible, without altering the value of n_v, to increase the value of n_r to the estimated value.

The 'snaking' tendencies of the model, which were more pronounced at small angles of incidence, could be greatly reduced by fitting an upper dorsal fin (described in section 5.7).

1. *Introduction.*—During recent flight tests on *Meteor* aircraft, a marked tendency was observed for self-excited lateral oscillations or 'snaking' to occur. Calculations consequently made of the lateral stability derivative n_r, based on full-scale records of oscillations in yaw, were found to differ widely from the theoretically estimated value. It was therefore thought desirable to develop a technique for measuring the value of the lateral stability derivative, n_r, experimentally in the wind-tunnel with the immediate objectives in view of:—

(*a*) comparing the results obtained in the wind-tunnel with corresponding values in flight;

(*b*) investigating what modifications could be made to the aircraft in order to reduce the lateral self-excited oscillations in flight.

Wind-tunnel measurements of n_r, which have been made in the past (R. & M. 580[1], R. & M. 932[2]) were based on the damped oscillation methods described in R. & M. 111[3] and R. & M. 78[4], or on measurements made on the whirling arm (R. & M. 1249[5]). No recent

---

[*] R.A.E. Report Aero. 2199, received 14th August, 1947.

(24240)   A

measurements of n_r, however, have been made in wind-tunnels in this country, though some work has been done in America[6]. A secondary objective of the work described herein was also to design suitable apparatus, and to evolve a wind-tunnel technique for making and analysing records which would enable reliable results to be obtained with sufficient accuracy and with a minimum of time and effort.

2. *Method.*—The general equation of motion of a damped system having rotational freedom in one plane and controlled by springs can be written, as an approximation, in the form:

$$I \frac{d^2\psi}{dt^2} + f \frac{d\psi}{dt} + j\psi = 0. \qquad \qquad \qquad \qquad \qquad \qquad \qquad (1)$$

In this equation the effects of the ' solid friction ' component of the friction in the supporting system independent of $d\psi/dt$, denoted by F, has been omitted. F is a step-function changing sign with the direction of angular velocity in such a way as to be always in opposition to the motion[7]. The effect on the results of these experiments due to the omission of this term in equation (1) is discussed below (section 6.2).

For an aircraft having freedom of movement only in yaw:—

$$\text{Damping couple,} f = - (N_r + N_{rf}) \frac{d\psi}{dt} \qquad \qquad \qquad \qquad \qquad (2)$$

$$\text{Restoring couple,} j = (UN_v + k) \psi. \qquad \qquad \qquad \qquad \qquad (3)$$

Substituting in (1) we have:

$$I \frac{d^2\psi}{dt^2} - (N_r + N_{rf}) \frac{d\psi}{dt} + [UN_v + k] \psi = 0 \qquad \qquad \qquad \qquad (4)$$

where I = moment of inertia of aircraft about its vertical axis of rotation.

Let $$\frac{(N_r + N_{rf})}{I} = - 2a$$

and $$\frac{(UN_v + k)}{I} = b'.$$

Then equation (4) may be rewritten as:

$$\frac{d^2\psi}{dt^2} + 2a \frac{d\psi}{dt} + b'\psi = 0. \qquad \qquad \qquad \qquad \qquad \qquad (5)$$

If $b' > a^2$ the second-order differential equation (5) represents a damped harmonic oscillation of decreasing amplitude and period, T, where:

$$T = \frac{2\pi}{\sqrt{(b' - a^2)}} \cdot \qquad \qquad \qquad \qquad \qquad \qquad \qquad \qquad (6)$$

The solution of equation (5) is:

$$\psi = e^{-at} [P \sin (b' - a^2)^{1/2} t + Q \cos (b' - a^2)^{1/2} t] \qquad \qquad \qquad (7)$$

where P and Q are arbitrary constants.

The ratio of amplitudes of successive oscillations at times $t = t_n$ and $t = t_{n+1}$ is approximately

$$\frac{\psi_{\max} (t = t_n)}{\psi_{\max} (t = t_{n+1})} = e^{at} . \qquad \qquad \qquad \qquad \qquad \qquad \qquad (8)$$

The value of the logarithmic decrement, a, may be obtained from experimentally recorded angles of yaw, drawn on a time-base, by plotting the natural logarithms of the amplitudes of oscillations against time and measuring the slope of the resulting straight line which is equal to $-a$ (assuming solid friction effects are small, cf. section 6.2).

Alternatively a much less accurate, but more rapid estimate of the logarithmic decrement (but one which was not used in calculating the results of these experiments) may be found from the record as follows:

From equation (8)

$$a = \frac{\log_e \psi_{max} (t = t_n) - \log_e \psi_{max} (t = t_n + \theta)}{\theta} \qquad \qquad \qquad \qquad (9)$$

where θ is the time interval between two selected peaks on the record, the amplitudes of which are measured from the record and substituted in (9) whence a may be found.

The total damping term expressed as a function of the logarithmic decrement is:

$$(N_r + N_{rf}) = -2Ia \qquad \qquad \qquad \qquad \qquad \qquad \qquad \qquad (10)$$

and the damping term due to the friction component dependent on $d\psi/dt$:

$$N_{rf} = -2Ia_f. \qquad \qquad \qquad \qquad \qquad \qquad \qquad \qquad (11)$$

Eliminating N_{rf} from (10) and (11) we obtain

$$N_r = -2I (a - a_f). \qquad \qquad \qquad \qquad \qquad \qquad \qquad (12)$$

The value of a is found as described above with the model in the wind tunnel with wind on and a_f is found from a similar test on the model at zero wind speed and with the tail of the model removed to reduce aerodynamic damping. It may be argued that it is not sufficiently accurate to determine the apparatus damping, a_f, by merely removing the fin of the model under test, since the remaining fuselage may produce appreciable damping. This is further discussed below (section 6.2.3).

N_r is then found from equation (12) when I has been measured.

Expressing equation (12) in non-dimensional form gives:

$$n_r = \frac{d (C_n)}{d \left(\dfrac{rb}{2U}\right)} = \frac{4N_r}{\rho U S b^2} = \frac{-8I}{\rho S b^2} \left[\frac{a - a_f}{U}\right] \qquad \qquad \qquad \qquad (13)$$

and hence the value of n_r may be calculated.

Substitution of the values a and b' in equation (6) gives the period of oscillation, T.

$$T = \frac{2\pi}{\left(\left[\dfrac{Un_v + k}{I}\right] - \left[\dfrac{N_r + N_{rf}}{2I}\right]^2\right)^{1/2}} \cdot \qquad \qquad \qquad \qquad (14)$$

If a test be made at zero wind speed, then $N_r \simeq 0$, and $N_v \simeq 0$ if the oscillations are small. Further if N_{rf} is neglected (which may be considered justifiable if k is made comparatively large), then

$$T = \frac{2\pi}{\sqrt{(k/I)}}$$

or

$$I = \frac{kT^2}{4\pi^2}. \qquad \qquad \qquad \qquad \qquad \qquad \qquad \qquad \qquad (15)$$

3

A*

Hence, for a given value of k, and by measurement of the period of oscillation of the model and its supports at zero wind speed, the value of I may be checked against the value found by the more accurate bifilar suspension method.

2.1. *Wind-Tunnel Speed*.—In order to represent on the scale model correctly the motion of the full-scale aircraft, the non-dimensional period of oscillation, *i.e.*, period multiplied by (U/b) is the important factor which should be maintained constant. In addition there may be a small effect due to differences in the degree of damping (*i.e.*, number of oscillations required to damp to half amplitude) but this would seem to be of only secondary importance, unless the damping of—or, in the case of self-excited oscillations, the rate of growth of—the oscillations is very large.

For this reason the non-dimensional factor UT/b was arranged to be the same for the wind-tunnel tests as the corresponding value measured experimentally in flight, where the periods of oscillation in yaw of the aircraft had been measured at different speeds.

Let suffices F and M refer to flight and model conditions respectively.

Then
$$\frac{U_F T_F}{b_F} = \frac{U_M T_M}{b_M}$$

or, for these tests, since $\dfrac{b_F}{b_M} = n = 5 \cdot 5$ (model-scale factor)

$$U_M T_M = \frac{U_F T_F}{5 \cdot 5} = X. \qquad .. \qquad .. \qquad .. \qquad .. \qquad .. \qquad .. \qquad .. \qquad (16)$$

Three full-scale flight speeds of 400, 300 and 200 m.p.h. E.A.S. were considered. The corresponding periods of the yawing oscillation had been measured in flight for each of these three speeds and are given in Table 1, together with the corresponding values of X calculated from equation (16).

TABLE 1

Periods of Yawing Oscillation Measured in Flight for Various Speeds and Corresponding Values of X

Full-scale speed m.p.h. E.A.S.	U_F ft/sec	Period of oscillation T_F sec	X
400	588	1·68	179
300	441	2·00	160
200	294	2·80	149

Rearrangement of equation (15) and combination with equation (16) yields:—

$$U_M = \frac{X}{2\pi} \sqrt{\frac{k}{I}} \qquad .. \qquad .. \qquad .. \qquad .. \qquad .. \qquad .. \qquad .. \qquad .. \qquad (17)$$

whence values of U_M may be obtained for each spring stiffness (alteration of which was made by use of two different springs and various spring arm lengths). The values of U_M, corrected for the blockage effect of the model in the tunnel, are set out in Tables 2 and 3 below.

4

TABLE 2

Tunnel Velocities Required for Different Spring Strengths for the Complete Model

$$I = 14\cdot50 \text{ slug ft}^2 \qquad U_M = \frac{X}{2\pi}\sqrt{\left(\frac{k}{I}\right)} = 0\cdot418X\sqrt{k}$$

Spring size	Position*	k	$\sqrt{k}$	U_F=588 ft/sec X=179	U_F=441 ft/sec X=160	U_F=294 ft/sec X=149
				U_M ft/sec	U_M ft/sec	U_M ft/sec
Large	L.6	21·64	4·65	39·7	31·0	28·9
	L.12	86·6	9·31	69·4	62·1	57·8
	L.18	195	13·96	104	93·1	86·6
	L.24	346	18·60	139	124	115
Small	S.6	56·4	7·53	56·1	50·2	46·8
	S.12	226	15·05	112	100	93
	S.18	510	22·58	168	150	140
	S.24	906	30·1	224	201	187

TABLE 3

Tunnel Velocities Required for Different Spring Strengths for Model without Tail Unit

$$I = 13\cdot45 \text{ slug ft}^2. \qquad U_M = \frac{X}{2\pi}\sqrt{\left(\frac{k}{I}\right)} = 0\cdot0434X\sqrt{k}$$

Spring size	Position*	k	$\sqrt{k}$	U_F=588 ft/sec X=179	U_F=441 ft/sec X=160	U_F=294 ft/sec X=149
				U_M ft/sec	U_M ft/sec	U_M ft/sec
Large	L.6	21·64	4·65	36	32·2	30
	L.12	86·6	9·31	72	64·4	60
	L.18	195	13·96	108	96·6	90
	L.24	346	18·60	144	129	120
Small	S.6	56·4	7·53	58·3	52·1	48·5
	S.12	226	15·05	116	104	96·9
	S.18	510	22·58	175	156	146
	S.24	906	30·1	233	208	194

Most of the spring settings above were used during these tests, but some of the higher velocities were impractical owing to the strength limitations of the model and its supports.

3. *Apparatus.*—The equipment can be divided into two main sections:—

(a) the apparatus which supported the model rigidly against pitching and rolling movement, but which permitted freedom of movement in yaw with, it was originally considered, a minimum of frictional damping, provision being made for a limited adjustment of the angle of incidence.

* The spring size is denoted by the letter L for the large spring (rate 7·21 lb/in.) and S for the small spring (rate 18·85 lb/in.) The figure following the letter signifies the radial distance in inches of the spring attachment point from the centre of oscillation of the model.

(b) A means of accurately and conveniently recording the oscillations in yaw of the model.

3.1. *Supporting Apparatus.*—A diagrammatic sketch of the apparatus is shown in Fig. 2, and some details in Fig. 3. The model was supported at the geometric centre of the tunnel at a point corresponding to the c.g. of the full-scale aircraft by means of a metal bracket containing the mechanism for the adjustment of incidence. This bracket was securely pinned into a large steel tube A, Fig. 3, which itself was mounted in two large diameter ball-races, the upper one being secured at the top end of an outer support tube, B, welded to a base-plate screwed to the tunnel working-section floor and braced by wires also attached to the floor.

The lower ball-race was mounted in a housing attached to a separate plate screwed to the underside of the floor turntable joists. Precautions were taken to protect both ball-races from grit and dust. The lower end of the support tube A (containing an adjustment for length) rested on top of a flat circular air-lubricated bearing mounted on a metal tripod which carried the entire weight of the model and the support tube A. The parts of the mounting below the floor of the tunnel can be clearly seen in Fig. 4.

A spring lever arm (Figs. 2, 3 and 4) was securely clamped to the support tube A about three feet above the air-bearing, and was controlled by a pair of identical helical steel springs opposing one another, attached by adjustable tensioners to fixed plates bolted to the underside of the tunnel flooring. The tensioners enabled the fore-and-aft centre-line of the model (in its equilibrium position) to be set parallel to the tunnel axis, and also ensured that the springs were in tension under all conditions of yaw of the model. The spring arm and plates were drilled at several corresponding radii so that different spring moment arms could be used.

It was thus possible for the model to oscillate freely in yaw with a minimum of friction damping, the oscillations being partly controlled by the springs which assisted in restoring the model to its central position.

3.2. *Recording Equipment.*—In view of the lack of recent experience, two different sets of recording gear were constructed to measure the oscillations of the model in the tunnel.

3.2.1. *Optical method.*—This method was employed in the experiments described in R. & M. 580[1]. For the present experiments a collimator was constructed and was mounted with its axis vertical on the tunnel working-section roof directly above the model. It consisted essentially of a 500 watt bulb mounted in a tubular housing provided with forced cooling. Light from this passed through a diaphragm and was focussed by an adjustable lens on to a minute hole. An image of this intensely illuminated hole was focussed, by means of a second adjustable lens, on to a mirror on the model itself; and thence either on to a logarithmic scale mounted on the tunnel wall or on to a moving film which was analysed after completion of the experiments.

Although this method was used at first and gave satisfactory results, it was found more tedious and inconvenient (due to the necessity of having the working area in darkness) than the recording drum method described below.

3.2.2. *Recording drum.*—The recording drum consisted of an electrically-driven rotating cylinder (Figs. 5 and 6) carrying a detachable strip of specially prepared heat sensitive paper, the whole assembly being rigidly mounted in a framework attached to the tunnel structure. A carriage, supporting a special small electrically-heated stainless steel pen, slid on two cylindrical rails running parallel to the axis of the cylinder. The pen was lightly pressed on to the paper by means of a fine spring. The carriage was moved along the rails by a radial arm fixed to the vertical rod C (Fig. 3), which was securely attached at its upper end to the model and passed coaxially down the support tube A. The movement of the carriage was thus proportional to the angular displacement in yaw of the model. It was necessary to use a separate rod C, and not the support tube A, to actuate the pen arm because of the appreciable error in recording the angular deflection of the model which would have been introduced by the

6

twist of the support tube A under the spring restoring forces. At one end of the drum a second electrically heated pen was mounted on the arm of an electric relay controlled by an accurate time clock. Every half-second the pen was pressed momentarily on to the paper and a time base was thus marked on the record.

In order to make the analysis of the records less tedious, a light box (Fig. 7), was constructed, on which the record could be firmly attached. Natural logarithms of the amplitude of the oscillations were read off directly on a set-square, graduated in natural logarithms, which registered against a slide at the base of the record.

4. *Procedure.*—A solid wooden model of the *Meteor* Mark F.III (Fig. 1), of which the leading particulars are given in Table 4, was weighed and balanced to find its c.g. position. Its moment of inertia, I, along its axis of yaw, was then measured by the bifilar suspension method, and corrected for the displacement of the c.g. of the model from the position corresponding to that on the full-scale aircraft.

The model was then mounted in the tunnel and, with no wind on, the frictional logarithmic decrement, a_f, was found by giving the model an initial displacement of about 10 deg in yaw and analysing the records obtained, as described in section 2. (Fig. 8, No. 1, is a typical record.) Two control springs of different stiffnesses and several spring moment arms were tested, as indicated in Tables II and III. The tail-unit was removed for these tests and the fuselage faired in, in order to reduce the air damping to a minimum (*cf.* section 6.2.3). It may be objected that the frictional logarithmic decrement (*i.e.*, that part of the apparatus damping, due to rolling friction in the ball-bearings and viscous friction in the air-bearing, which is proportional to $d\psi/dt$) obtained in this way may not be the same for the various conditions of tests, because of the drag forces acting on the ball-bearings and variations in frictional forces of the air-bearing as the vertical load on it is reduced by lift forces on the model. It was thought that the latter effect would be small, but a check on the former was made by applying large drag loads through an additional ball-race. No change in the logarithmic decrement was discernible. The results of these tests are discussed in section 6.2.

A check on the moment of inertia of the model about its axis of yaw was also obtained by measuring the frequency of the oscillations and substituting values obtained in equation (15).

The model was next given displacements in yaw at various wind speeds corresponding to the type of spring and spring arm length set out in Tables 2 and 3 (*see* Fig. 8, Nos. 2 and 3 for reproduction of the type of record obtained). Four complete sets of experiments were made with the model set at angles of incidence $-0\cdot4$, 1, 2 and $4\cdot5$ deg. Various modifications, listed below, were then made to the model and some values of n_r obtained for each case.

In addition some tests were also made with the restoring springs removed. The model was then free to oscillate in yaw in a manner simulating to some degree the actual flight conditions. These tests are referred to in this report as ' free runs ' and give some indication in a recorded form (*see* Fig. 9) of the snaking characteristics of the model in each condition. Since the model was not a dynamically similar one, the results obtained in this way are of only comparative value.

The model was tested in all cases with the transition fixed on the wings at 10 per cent of the chord behind the leading edge by means of wires on both the upper and lower surfaces. The liquid film evaporation method[7] was used to check that the transition did, in fact, take place at the wires.

The stiffnesses of the restoring springs were measured by normal methods.

5. *Conditions Under which Model was Tested.*—Values of n_r and records of ' free runs ' were obtained in the following cases:—

5.1. *Case A. Flow Through Nacelles Represented. Standard Model.*—The results of these tests are not included in this report because it was found that, on tufting the entries to the

7

nacelles, there was an irregular breakaway near the lip which might have accentuated the unsteadiness in yaw of the model. As it appeared to be impossible that such a breakaway occurred on the full-scale aircraft, the nacelles were blocked up and faired to a point at their downstream end.

5.2. *Case B. Nacelles Blocked and Faired. Standard Case.*—Photographs of the model in this condition are shown in Figs. 10 and 11. A large number of values of n_r were measured for four angles of incidence, *i.e.*,—0·4, 1, 2 and 4·5 deg.

5.3. *Case C. Complete Tail Unit Removed and Fuselage Faired. Model as for Case B.*— Some tests were made with the model in this condition to measure the contribution of the fin at the three incidences.

5.4. *Case D. Transition Wires on Both Sides of the Fin at* 0·1c. *Model as for Case B.*—In order to find out if the snaking tendency of the model might be reduced by fixing the transition on the fin at some definite point, two wires were glued to each side of the fin at 0·1c. Tests were made at the same angles of incidence as for Case C.

5.5. *Case E. Cord on Trailing Edge of Fin. Model as for Case B.*—A cord of overall width 1·25 in. and of total length 3 ft 3 in., extending 15 in. above, to 2 ft below, the tailplane had been fitted in flight to reduce the snaking tendency and a scale version was therefore fitted to the model for all the subsequent tests. The same incidence range as for Case C was used.

5.6. *Case F. Propellers Fitted. Model as for Case E.*—The possibility that the effect of an asymmetric slipstream might make an alteration to the value of n_r was thought worth investigating. It was not possible to use powered propellers, so three-bladed freely windmilling propellers of 10 ft 9 in. diameter full-scale were fitted (Figs. 12 and 13). Values of n_r were measured for the four angles of incidence of Case B.

5.7. *Case G. Dorsal Fin Fitted on Top of Fuselage.* (*Propellers on Model as for Case F.*)— A dorsal fin (Fig. 14) was attached to the model in an attempt to increase the effectiveness of the fin. The dorsal fin extended from beneath the acorn on the fin to a point on the top of the fuselage 3 ft 9 in. full-scale in front of the original fin-fuselage junction.

5.8. *Case H. Additional Lower Dorsal Fin Attached. Model as for Case G.* (*Propellers On.*)— The fin area was further increased by extending the lower part of the fin (Fig. 15) to a point on the lower side of the fuselage 4 ft full-scale, forward of the original fin-fuselage junction point.

5.9. *Case J. With Upper and Lower Dorsal Fins but Propellers Removed and Model as for Case E.*—It was thought desirable to find the effect of the dorsal fins on the behaviour of the model under conditions similar to Case E. A few tests were therefore made for the three angles of incidence —0·5, 2 and 4·5 deg.

5.10. *Case K. Strakes Fitted to Rear Part of the Fuselage. Model as for Case F.*—In order to reduce circulation of flow round the fuselage in the region of the fin when the aircraft was yawed, a single strake 3 in. in height, full-scale, extending from above the trailing edge of the wing to the leading edge of the fin, was fitted, in the first place, along the top of the fuselage. In addition, the effect of two strakes running over the sides of the fuselage was tested.

5.11. *Case L. Other Tests.*—An unusual modification to the aircraft, which was tested in flight, was to fix a $\frac{5}{8}$-in. diameter rope round the fuselage just forward of the cockpit. This had been found to decrease the snaking tendency. A piece of rubber-insulated wire representing to scale a $\frac{5}{8}$-in. diameter rope was therefore fixed on the model, and a few values of n_r and ' free runs ' obtained at the incidences at which the model normally oscillated most violently. A typical record of a free run is to be seen in Fig. 9, No. 7. An improvement similar to that found in flight was obtained on the model.

8

Besides the tests already described, several others of a rather unscientific nature were tried, but are not included in this report, because they did not produce any appreciable improvements. The model was also fully tufted in order to see if any breakaways occurred or whether any bad flow characteristics could be found.

The results of the measurements of n_r are set out in Tables 5, 6 and 7. These tables give the values of the frictional logarithmic decrement, total logarithmic decrements, corresponding values of n_r and tunnel speeds for each spring position at each angle of incidence tested.

6. *Discussion of Results.*—6.1 *Introduction.*—Two papers[8, 9] have been written concerning this report since its appearance in its original form. These reports offered constructive criticism, particularly Ref. 9, which raised several points of importance which led the present authors further to consider their original results and to record their conclusions in Ref. 10.

For the sake of completeness, the findings of the further analysis of the results, given in full in Ref. 10, will be referred to in the present discussion together with some points of importance raised in Refs. 8 and 9. All results, however, given in Tables 5, 6 and 7 and plotted in Fig. 16 are those originally obtained, and have not been corrected for ' solid friction ' effects described below.

6.2. *Sources of Inaccuracy in Experiments.*—6.2.1. *Effect of solid friction.*—Refs. 9 and 11 indicate the importance of allowing for 'solid friction' (*i.e.*, the friction term independent of $d\psi/dt$ when evaluating results of damped oscillation experiments. The effect, as has already been indicated in section 2, is to add to the equation of motion a step-function, F, which changes sign with the direction of angular velocity in such a way as always to oppose the motion.

Equation (1) then becomes,

$$I \frac{d^2\psi}{dt^2} - (N_r + N_{rf}) \frac{d\psi}{dt} + (UN_v + k)\psi \mp F = 0. \qquad .. \qquad .. \qquad .. \qquad (18)$$

It can be shown that the amplitude of ψ_n of the nth peak is given by

$$\psi_n = (\psi_0 + B) e^{-n\delta/2} - B \qquad .. \qquad .. \qquad .. \qquad .. \qquad .. \qquad .. \qquad .. \qquad (19)$$

where $\delta = aT$

and $$B = \frac{F}{(UN_v + k)} \cdot \frac{(1 + e^{-\delta/2})}{(1 - e^{-\delta/2})} \cdot \qquad .. \qquad .. \qquad .. \qquad .. \qquad .. \qquad .. \qquad (20)$$

The equation of the curve, drawn through the points of peak amplitude on the record of amplitude against time, will differ from the pure exponential by a constant which contains the step-function F. The curves of $\log_e$ (amplitude) against n or t should therefore no longer be linear. The effect of F may easily be eradicated, and the results thereby corrected, by adding constant amounts to the measured amplitudes until the curve of $\log_e$ (amplitude) against n does become linear. The slope of the resulting straight line should then give the correct value of δ or a.

6.2.2. *Partial re-analysis of results.*—No allowance had been made during the original analysis for the effects of solid friction described in section 6.2.1 because it had been assumed in the first place that equation (1) was sufficiently accurate. Furthermore, in support of this assumption, the original curves of $\log_e$ (amplitude) on a time basis, although not all linear, showed no systematic downward curvature which is symptomatic of the presence of solid friction. Any deviations from a straight line were attributed to the snaking tendencies of the model. In the light of the points raised in Ref. 9 some of the results have therefore been analysed again to investigate the solid friction effect in greater detail.

9

In Fig. 17 are plotted some curves of $\log_e (\psi_n + \psi_{n+1})$ against n at $\alpha = -0\cdot4$ and $4\cdot5$ deg at various wind speeds. Also shown are the straight lines that can be obtained by adding in each case a constant quantity B to ψ_n. The evaluation of the results found by using the corrected straight lines are given in Table 9. The effect of solid friction is difficult to estimate at $\alpha = -0\cdot4$ deg because self-excited oscillations of the model tend to mask its effects. At $\alpha = 4\cdot5$ deg, where the movement of the model in yaw was much steadier, the friction appears to be much smaller (less than $0\cdot01$ lb-ft) and in cases (G) and (H) the effect even appears to be in the opposite direction. It has not been found possible to re-analyse a sufficient number of reliable records, to estimate exactly the effect which the correction for solid friction would have on the value of n_r. The results obtained in the re-analysis are very scattered: but they indicate, together with evidence obtained on other tests with this apparatus for another aircraft, that the original results, given in this report in Tables 5, 6 and 7 and plotted in Fig. 16, should be not more than 5 per cent in excess of the results fully corrected for solid friction effect.

The conclusions of Ref. 9 would indicate that this figure is of the order of 25 per cent high. It should be pointed out that this conclusion is based entirely on one experimental record, shown in Fig. 8 of this report, which by chance happens to be unrepresentative of the main body of tests, part of which has been re-analysed, as described above, to show the conclusion of the preceding paragraph.

6.2.3. *Further investigation into the effect of drag force on friction*.—Before the original tests were started, a large drag load had been applied through a third ball-race, as described under section (4). No apparent change in the logarithmic decrement was discernible at the time, but in view of subsequent suggestions of the importance of the solid friction effects on the accuracy of the results, it was considered advisable to investigate directly the effect of the drag on the friction of the bearings. Further rests were therefore made after the completion of the experiments described in this report. They were conducted, outside the tunnel, during July 1948, in connection with similar tests to those on the *Meteor* for another aircraft 'A'. In place of the model 'A' a steel bar weighted to give the same moment of inertia about the axis of yaw was used. Various lateral forces were applied to the supporting tube by means of a third ball-race and a horizontal wire. A range of periods of oscillation was covered and the drag force was varied from 0—37 lb in each case. From the records thus obtained, the solid friction, F, and the frictional damping factor, a_f, were calculated. The results are given in Table 10 and plotted against drag force in Fig. 18.

It will be seen that the solid friction is extremely variable; but it is of the same order as that estimated from re-analysis of previous tests in the tunnel. For drag forces of less than 10 lb (the maximum drag of the *Meteor* model in the tunnel was about 7 lb) the greatest value of F was $0\cdot02$ lb-ft as opposed to about $0\cdot03$ lb-ft in the tunnel. For higher drags the solid friction shows a definite increase, as indicated by the dotted lines in Fig. 18a, but the scatter about these lines is very great. The curves of the frictional damping factor a_f against drag, Fig. 18b, show that the assumption, made in section (4) above that a_f is constant, is probably justifiable; but again there is a large amount of scatter.

By comparing the values of a_f for the *Meteor* (Table 5) with the results obtained in these subsidiary tests (Table 10) at the most nearly corresponding periods of oscillation, it is seen that the near values of a_f given here are considerably smaller than those originally measured. This reduction is not entirely due to the solid friction correction, however, and it is probable, therefore, that the air damping on the model had a fairly large effect in spite of the statement made to the contrary in Reference 6. It is interesting to note that the effect of such a reduction in a_f would be to counteract almost exactly the solid friction correction.

It would seem advisable, therefore, as suggested in Ref. 9, that in future, for measurements of frictional damping, the model should be replaced by a metal bar of minimum dimensions to give the same moment of inertia as the model about its axis of yaw.

10

6.3. *Convenience of Technique.*—It was found that the experimental technique described in this report enabled measurements of n_r to be made with reasonable accuracy and comparative ease. It is interesting to note that the complete making and analysing of one record occupied 25 minutes of which the major portion was devoted to analysis and calculations.

6.4. *Measurements of n_r.*—It may be seen from Table 5 that there was a considerable variation amongst the results obtained for a particular incidence: where the self-excited oscillations of the model became more pronounced and interfered with the normal decay of the damped oscillations the discrepancies became larger.

The results for Case B, the standard case, for a *Meteor* Mk. F.III aircraft, are given in Table 5 and mean values of n_r for each incidence are plotted against corresponding values of C_L in Fig. 16.

An estimate for the complete model (*see* Ref. 6) gives:

$$n_r = -\left[2\frac{l}{b}\,\Delta n_{v\,(\text{tail})}\right] - \left[0\cdot33\left\{\frac{1+3\lambda}{2+2\lambda}\right\}C_{D0} + 0\cdot20\left\{1 - \frac{AR-6}{13} - \frac{1-\lambda}{2\cdot5}\right\}C_L{}^2\right] \qquad (21)$$

For the *Meteor* model under consideration this becomes

$$n_r = -\ 0\cdot106 - 0\cdot003 - 0\cdot18C_L{}^2 \text{ (for complete model)}$$

or $\qquad n_r = -\ 0\cdot003 - 0\cdot18C_L{}^2$ (for model without tail-unit).

Values of $-n_r$ obtained for the values of C_L used in these tests are plotted in Fig. 16. Equation (21) would indicate that curves of $-n_r$ plotted against C_L should be of parabolic form with a minimum at $C_L = 0$. It will be seen, however, from Fig. 16 that the experimental minimum values of $-n_r$ occur at a small positive C_L of about $0\cdot15$. It is suggested in Ref. 6 that this is due to the possibility that, for an overall value of $C_L = 0$, the lift is not uniformly zero over the whole wing, and therefore the wing contribution to $-n_r$ would also not be zero, and thus $-n_r$ would not have its minimum value at an overall value of $C_L = 0$. The value given by equation (21) for the complete aircraft is about 20 per cent greater than the measured value for the standard case, but agrees well with the values for cases G and H (with dorsal fins).

6.4.1. *Agreement with Flight Tests.*—As stated earlier, the wind-tunnel technique here described was instigated because of the wide difference originally obtained between the theoretical estimate and the flight tests. It was subsequently found that the large discrepancy was due to a number of assumptions which had to be made in the first place in computing the flight results. The pedal-fixed conditions of the tests were at first considered as representing rudder-fixed conditions, but later it was proved that the rudder was moving sufficiently to affect the damping of the aircraft. By taking into account that, under flight conditions, all three degrees of freedom of motion were involved the discrepancy was still further reduced.

Comparison of the damping of the lateral oscillations as estimated from tunnel tests (uncorrected for solid friction effects) with the final values measured in flight at low speeds showed that the latter were about 10 per cent less than the former. Application of the correction for solid friction and apparatus damping (*see* section 6.2) would, it is thought, not appreciably alter this result. This discrepancy may not represent a difference in the value of n_r, as other errors in y_v and rolling effects are involved.

It may be concluded that the agreement is very satisfactory, considering the difficulties involved.

The discrepancy between flight and tunnel results increases with speed. This is possibly due to the effect of unsteady flow at higher Mach numbers, an effect which will not be covered by the wind-tunnel tests.

11

6.4.2. *Effect of modifications to the model on n_r.*—Experiments with the tail-unit removed, Case C, gave values of $-n_r$ which are shown in Table 6 and plotted in Fig. 16. Although the minimum value occurs at $C_L = 0 \cdot 15$, the shape of the curve is in good agreement with the wing contribution indicated by equation (21).

Tests of Case D, with the transition fixed at $0 \cdot 1c$ on both sides of the fin, gave a slight reduction of $0 \cdot 005$ on the value of $-n_r$. Subsequent tests were made with the wires removed.

The fitting of a cord, described in section 5.5, on the trailing edge of the fin, Case E, gave a slight increase in the value of $-n_r$ of about $0 \cdot 005$. Since flight tests had been made with this cord in position all further tests were made with the model in this condition.

The tests on the model fitted with windmilling propellers, Case F, were made to investigate the possibilities that an asymmetric slip-stream might have an effect on n_r. No change was perceptible, but it is interesting to note that, in this case, the minimum value of n_r occurs at $C_L=0$.

The effect of fitting top and bottom dorsal fins was investigated in Cases G and H. Fig. 16 shows that a considerable increase in $-n_r$ of $0 \cdot 01$ to $0 \cdot 015$ over the previous Case F was obtained with both fins fitted. The fins were also tested separately and it was found that the contribution of the bottom dorsal fin was negligible. Since this simple modification appeared so effective, further tests were made with the propellers removed and the model tested as for Case E. The improvement was found to be even greater than with propellers fitted.

The effect of wrapping a $\frac{5}{8}$-in. diameter rope round the fuselage was investigated. A few values of n_r were measured but no increase over the value for Case E was detected.

Ref. 10 points out that the forces on the nacelles may be modified considerably due to the flow through the ducts. It was not possible to represent correctly the flow through the ducts during the present tests, but it is possible that this might be an important factor which should be further investigated.

6.5. *'Snaking' Characteristics of the Model.*—The results of these tests are given in Table 8 and some examples of records are given in Fig. 9.

In the standard Case B, bad oscillations (± 1 deg) took place at low angles of incidence (Fig. 9, Nos. 1 and 2) but almost completely disappeared at the largest angle of incidence tested, $4 \cdot 5$ deg, (Fig. 9, No. 3).

The fitting of the top and bottom dorsal fins, Cases G and H, greatly reduced the amplitude of the snaking oscillation (Fig. 9, Nos. 4, 5 and 6).

The effect of attaching propellers, Case F (Fig. 9, No. 8) indicated that little improvement had been obtained.

The fitting of strakes, Case K, very slightly improved the snaking tendencies.

The result of wrapping a $\frac{5}{8}$-in. diameter rope (full-scale) round the fuselage in front of the cockpit, Case L, was, rather surprisingly, to produce as great an improvement in the snaking characteristics (Fig. 9, No. 7) as the fitting of dorsal fins.

6.6. *Investigation of the Flow Round the Model.*—Observations of tufts on the model showed that there were no irregular breakaways in general. A slight breakaway of flow beneath the fuselage behind the wing at small angles of incidence was, however, detected. It is not considered that this could have been responsible for the snaking tendencies of the model; and other evidence confirms that possible unsteadiness of tunnel flow was not the cause.

7. *Recommendations.*—7.1. *Experimental Technique.*—The experimental technique described here is considered to be very satisfactory, but it is thought that some scatter of the results might be reduced by improvement of the mechanical details of the test, although Ref. 10 suggests that part of the scatter is probably inherent in this kind of experiment because of transient phenomena in the boundary layer which affect the restoring moment.

12

It is, however, suggested that ball-bearings, which have been used here to take horizontal loads are not reliable, and if any further work is contemplated, these should be replaced by some form of cylindrical air-lubricated bearings, which should reduce the solid friction to a negligible level. This would have the additional considerable advantage that the analysis, involving solid friction corrections, would be much reduced.

The vertical load may be taken by an air-bearing similar to the one described here, but the use is recommended of a long thin high tensile supporting wire attached at one end to the model at a point on the axis of yaw.

7.2. *Modifications to Meteor Aircraft.*—It might be profitable to make flight tests with an upper dorsal fin of similar dimensions to that described in this report fitted to a Standard Mark F. III *Meteor*. The tests indicate that an increase in the value of $-n_r$ of about $0\cdot015$ might be obtained, and also the snaking tendencies of the aircraft considerably reduced.

7.3. *Further Wind-Tunnel Tests.*—It is thought that the snaking may be due to a peculiar ineffectiveness of the fin at very small angles of yaw ($\psi < \pm 1$ deg). It is suggested that wind-tunnel measurements of n_v at small angles of yaw might be made to investigate this possibility. Curves of C_n versus β might also be obtained to see if any discontinuities in the curve near the position of zero yaw were present.

8. *Acknowledgments.*—The authors wish to express their thanks to Mr. W. H. C. Maloney for his help in designing the test-rig and recording equipment, and to Mr. L. W. Bryant of the National Physical Laboratory for his advice and criticism.

REFERENCES

No.	Author	Title, etc.
1	G. P. Douglas	Measurement of the Derivatives M_q and N_r for a Number of Aeroplane Models. R. & M. 580. January, 1919.
2	R. A. Fraser, A. S. Batson and A. G. Gadd.	Experiments on a Model of a Bristol Fighter Aeroplane (1/10 scale). Section 2. Lateral Derivatives by the Forced Oscillation Method. R. & M. 932. October, 1924.
3	F. H. Bramwell and E. F. Relf	Experiments on Models of Complete Aeroplanes—IV. Determination of the Pitching Moment due to Pitching for a Model Biplane at Various Inclinations to the Wind. R. & M. 111. March, 1914.
4	L. Bairstow and L. A. MacLachlan	The Experimental Determination of Rotary Coefficients. R. & M. 78. 1913.
5	L. W. Bryant and A. S. Halliday	Measurement of Lateral Derivatives on the Whirling Arm. R. & M. 1249. March, 1929.
6	J. P. Campbell and W. O. Matthews	Experimental Determination of the Yawing Moment due to Yawing Contributed by the Wing, Fuselage and Vertical Tail of a Midwing Airplane Model. A.R.C. Report 7205. November, 1943. (Unpublished.)
7	W. E. Gray	A Simple Visual Method of Recording Boundary Layer Transition (Liquid Film). A.R.C. 10,028. August, 1946. (Unpublished.)
8	V. M. Falkner	Notes on A.R.C. Reports 10,785 and 10,786. Measurements of Yawing Moment due to Yawing. A.R.C. Report 10,978. November, 1947. (Unpublished.)
9	P. T. Fink	Notes on the Experimental Results of A.R.C. Reports 10,785 and 10,786. Measurement of Yawing Moment due to rate of Yaw. A.R.C. Report 11,161. January, 1948. (Unpublished.)
10	R. C. Lock and J. G. Ross	Notes on Measurement of Yawing Moment due to Yawing. (A.R.C. Reports 10,785 and 10,786). A.R.C. Report 11,961. November, 1948. (Unpublished.)
11	J. M. Evans and P. E. Fink	Stability Derivatives. Determination of l_p by Free Oscillations. Report ACA–34. April, 1947.

LIST OF SYMBOLS

n_r Rate of change of yawing moment coefficient with yawing angular velocity per unit of

$$\frac{rS}{U}\left(\partial C_n/\partial\left(\frac{rS}{U}\right)\right) = \frac{4N_r}{\rho USb^2}$$

n_v Rate of change of yawing moment coefficient with angle of side-slip, $-(\partial C_n/\partial\psi)$

C_L Lift coefficient, (L/qS)

C_n Yawing moment coefficient, $\left(\dfrac{N}{qSb}\right)$

N Yawing moment, ft-lb

N_r Rate of change of aerodynamic yawing moment with yawing angular velocity, $(\partial N/\partial r)$

N_{rf} Rate of change of frictional yawing moment with yawing angular velocity, $[(\partial N/\partial r)_f]$

α Angle of incidence, degrees

k Rate of change of restoring moment of helical springs with angle of yaw

L Lift, lb

q Dynamic pressure, $(\frac{1}{2}\rho U^2)$, lb/ft²

S Wing area, ft²

r Yawing angular velocity, radn/sec

b Span of wing, ft

b_F Span of wing, full-scale, ft

b_M Span of wing of model, ft

U Wind speed, ft/sec

U_F Wing speed full-scale, ft/sec

U_M Tunnel wind speed, ft/sec

ρ Density of air, slugs/ft³

ψ Angle of yaw, radn

a Total logarithmic decrement of damping factor

a_f Logarithmic decrement due to friction

t Time, sec

T Period of yawing oscillation, sec

T_F Period of yawing oscillation, full-scale, sec

T_M Period of yawing oscillation of model, sec

f Damping-force/unit-velocity

j	Constraining-force/unit-angle of yaw
I	Moment of inertia of aircraft about vertical axis of rotation in yaw, slugs-ft^2
b'	Constant (*see* section 2)
P, Q	Arbitrary constants
W	Weight, lb
K	Radius of gyration, ft
n	Model-scale factor
g	Acceleration due to gravity, ft/sec^2
AR	Aspect ratio
λ	Taper ratio $=$ tip-chord/root-chord
X	Factor $= \dfrac{U_F T_F}{b_F} = \dfrac{U_M T_M}{b_M}$
C_{D0}	Profile-drag coefficient

TABLE 4

*Leading Particulars of Meteor Aircraft Mark F. III (Standard Case)
and relevant model data*

Model scale: 1/5·5

Wing:	Full-scale	Model
Gross Area S ft²	374	12·36
Wing span b ft	43	7·82
S.M.C. c ft	8·71	1·58
Wing root chord ft	11·68	2·12
Wing aspect ratio	4·94	4·94
Wing-body setting deg	1·0	1·0
Dihedral		
Centre-plane spar datum	0° 52½′	0° 52½′
Outer–plane spar datum	6° 0′	6° 0′

Tail Unit:		
Tailplane area ft²	61	2·02
Tailplane incidence (short nacelles)	0°	0°
Fin and rudder total area ft²	42·4	1·40
Rudder total area ft²	19·0	0·63
Fin arm	23·0 ft	4·18
Fin volume coefficient	0·059	0·059

Other particulars:		
Actual weight of aircraft	11,000 lb.	(≡64·9 lb)
Actual weight of model		150 lb
Moment of inertia about full-scale c.g. position:		
Without tail-unit slugs–ft²		13·45
Standard case slugs–ft²		14·57
Standard case with propellers slugs–ft²		14·70
Actual radius of gyration about full-scale c.g. (mean)	8·1 ft	(≡1·47 ft)
,, ,, ,, ,, of model about c.g.		1·75 ft

Restoring spring stiffness:	
Large spring	7·22 lb/in.
Small spring	18·88 lb/in.

TABLE 5

Values of the Logarithmic Decrements, Tunnel Speeds and n for the Standard Case B

α deg	C_L	Mean value of n_r	Spring position	Group I					Group II					Group III				
				a	a_f	$a-a_f$	U (ft/sec)	$-n_r$	a	a_f	$a-a_f$	U (ft/sec)	$-n_r$	a	a_f	$a-a_f$	U (ft/sec)	$-n_r$
−0·4	0	−0·091	L 6	0·075	0·020	0·055	34·7	0·107	0·069	0·020	0·049	31·1	0·106	0·063	0·020	0·043	28·9	0·100
			L 12	0·097	0·011	0·086	69·4	0·084	0·096	0·011	0·085	62·1	0·092	0·088	0·011	0·077	57·8	0·090
			L 18	0·145	0·011	0·134	104·0	0·087	0·138	0·011	0·127	93·1	0·092	0·115	0·011	0·104	86·6	0·081
			L 24	0·189	0·011	0·178	138·6	0·087	0·176	0·011	0·165	123·6	0·090	0·151	0·011	0·140	115·4	0·082
			S 6	0·100	0·019	0·081	56·1	0·097	0·087	0·019	0·068	50·2	0·091	0·078	0·019	0·059	46·8	0·085
			S 12	0·162	0·016	0·146	112·2	0·088	0·168	0·016	0·152	100·6	0·102	0·142	0·016	0·126	93·4	0·091
			S 18	—	—	—	—	—	0·212	0·016	0·196	150·4	0·088	0·174	0·016	0·158	140·1	0·076
1·0	0·06	−0·087	L 6	0·070	0·020	0·050	34·7	0·097	—	—	—	—	—	—	—	—	—	—
			L 12	0·105	0·011	0·094	69·4	0·091	0·094	0·011	0·083	62·1	0·090	0·093	0·011	0·082	57·8	0·096
			L 18	0·130	0·011	0·119	104·0	0·077	0·140	0·011	0·129	93·1	0·094	0·120	0·011	0·109	86·6	0·085
			L 24	0·164	0·011	0·153	138·6	0·075	0·180	0·011	0·169	123·6	0·092	0·145	0·011	0·134	115·4	0·078
			S 6	0·099	0·019	0·080	56·1	0·096	0·091	0·019	0·072	50·2	0·097	0·085	0·019	0·066	46·8	0·095
			S 12	0·167	0·016	0·151	112·2	0·091	0·130	0·016	0·114	100·6	0·077	0·121	0·016	0·105	93·4	0·076
			S 18	—	—	—	—	—	0·190	0·016	0·174	150·4	0·078	0·170	0·016	0·154	140·1	0·074
2·0	0·18	−0·076	L 6	0·070	0·020	0·050	34·7	0·097	0·060	0·020	0·040	31·1	0·087	0·056	0·020	0·036	28·9	0·084
			L 12	0·087	0·011	0·076	69·4	0·074	0·080	0·011	0·069	62·1	0·075	0·077	0·011	0·066	57·8	0·077
			L 18	0·126	0·011	0·115	104·0	0·074	—	—	—	—	—	—	—	—	—	—
			L 24	—	—	—	—	—	—	—	—	—	—	—	—	—	—	—
			S 6	0·077	0·019	0·058	56·1	0·070	0·081	0·019	0·063	50·2	0·085	0·080	0·019	0·061	46·8	0·088
			S 12	0·129	0·016	0·113	112·2	0·068	0·119	0·016	0·103	100·6	0·070	0·113	0·016	0·097	93·4	0·070
			S 18	—	—	—	—	—	0·168	0·016	0·152	150·4	0·068	0·173	0·016	0·157	140·1	0·076
4·5	0·35	−0·093	L 6	0·069	0·020	0·049	34·7	0·095	0·066	0·020	0·046	31·1	0·100	0·065	0·020	0·035	28·9	0·082
			L 12	0·109	0·011	0·098	69·4	0·095	0·100	0·011	0·089	62·1	0·097	0·094	0·011	0·083	57·8	0·097
			L 18	0·153	0·011	0·142	104·0	0·092	0·136	0·011	0·125	93·1	0·091	0·134	0·011	0·123	86·6	0·096
			L 24	0·190	0·011	0·179	138·6	0·087	0·178	0·011	0·167	123·6	0·091	0·170	0·011	0·159	115·4	0·093
			S 6	0·099	0·019	0·080	56·1	0·096	0·090	0·019	0·071	50·2	0·095	0·086	0·019	0·067	46·8	0·097
			S 12	0·168	0·016	0·152	112·2	0·091	0·147	0·016	0·131	100·6	0·088	0·142	0·016	0·126	93·4	0·091
			S 18	—	—	—	—	—	0·214	0·016	0·198	150·4	0·089	0·206	0·016	0·190	140·1	0·092

17

TABLE 6

Values of the Logarithmic Decrements, Tunnel Speeds and n_r for the Various Conditions of the Model Tested. Cases C, D and E

Description of test	α deg	C_L	Mean value of n_r	Spring position	Group I					Group II					Group III				
					a	a_f	$a-a_f$	U (ft/sec)	$-n_r$	a	a_f	$a-a_f$	U (ft/sec)	$-n_r$	a	a_f	$a-a_f$	U (ft/sec)	$-n_r$
C. Without tail unit	−0·5	0	−0·007	L 12	0·022	0·011	0·011	72·0	0·010	0·019	0·011	0·008	64·4	0·008	0·018	0·011	0·007	60·0	0·007
				S 12	0·024	0·016	0·008	116·4	0·004	0·026	0·016	0·010	104·1	0·006	0·025	0·016	0·009	96·9	0·006
	2·0	0·18	−0·003	L 12	0·016	0·011	0·005	72·0	0·004	0·016	0·011	0·005	64·4	0·005	0·016	0·011	0·005	60·0	0·005
				S 12	0·022	0·016	0·006	116·4	0·003	0·020	0·016	0·004	104·1	0·002	0·018	0·016	0·002	96·9	0·001
	4·5	0·35	−0·011	L 12	0·026	0·011	0·015	72·0	0·013	0·024	0·011	0·013	64·4	0·013	0·023	0·011	0·012	60·0	0·012
				S 12	0·034	0·016	0·018	116·4	0·010	0·031	0·016	0·015	104·1	0·009	0·030	0·016	0·014	96·9	0·009
D. With transition wires on fin and rudder	−0·5	0	−0·082	L 12	0·094	0·011	0·083	69·4	0·081	0·093	0·011	0·082	62·1	0·089	0·086	0·011	0·075	57·8	0·088
				S 12	0·149	0·016	0·133	112·2	0·080	0·136	0·016	0·120	100·2	0·081	0·120	0·016	0·104	93·4	0·075
	2·0	0·18	−0·072	L 12	0·084	0·011	0·073	69·4	0·071	0·080	0·011	0·069	62·1	0·075	0·076	0·011	0·065	57·8	0·076
				S 12	0·120	0·016	0·104	112·2	0·063	0·127	0·016	0·111	100·2	0·075	0·111	0·016	0·095	93·4	0·069
	4·5	0·35	−0·091	L 12	0·105	0·011	0·094	69·4	0·091	0·096	0·011	0·085	62·1	0·092	0·092	0·011	0·081	57·8	0·095
				S 12	0·163	0·016	0·147	112·2	0·088	0·148	0·016	0·132	100·2	0·089	0·143	0·016	0·127	93·4	0·092
E. With cord on rudder	−0·5	0	−0·092	L 12	0·101	0·011	0·090	69·4	0·088	0·093	0·011	0·082	62·1	0·089	0·094	0·011	0·083	57·8	0·097
				S 12	0·163	0·016	0·147	112·2	0·088	0·160	0·016	0·144	100·2	0·097	0·141	0·016	0·125	93·4	0·090
	2·0	0·18	−0·086	L 12	0·100	0·011	0·089	69·4	0·087	0·096	0·011	0·085	62·1	0·092	0·085	0·011	0·074	57·8	0·086
				S 12	0·155	0·016	0·139	112·2	0·084	0·139	0·016	0·123	100·2	0·082	0·133	0·016	0·117	93·4	0·084
	4·5	0·35	−0·101	L 12	0·116	0·011	0·105	69·4	0·102	0·108	0·011	0·097	62·1	0·105	0·102	0·011	0·091	57·8	0·106
				S 12	0·181	0·016	0·165	112·2	0·099	0·163	0·016	0·147	100·2	0·099	0·150	0·016	0·134	93·4	0·097

TABLE 7

Values of the Logarithmic Decrements, Tunnel Speeds and n_r for the Various Conditions of the Model Tested. Cases F, H, J and L

Description of test	α deg	C_L	Mean value of n_r	Spring position	a	a_f	$a-a_f$	U (ft/sec)	$-n_r$	a	a_f	$a-a_f$	U (ft/sec)	$-n_r$	a	a_f	$a-a_f$	U (ft/sec)	$-n_r$
F. With propellers on (and cord on rudder)	−0·5	0	−0·089	L 12	0·102	0·011	0·091	69·4	0·089	0·095	0·011	0·084	62·1	0·092	0·089	0·011	0·078	57·8	0·092
				S 12	0·158	0·016	0·142	112·2	0·086	0·140	0·016	0·124	100·2	0·084	0·139	0·016	0·123	93·4	0·090
	2·0	0·18	−0·090	L 12	—	—	—	—	—	0·097	0·011	0·086	62·1	0·094	0·090	0·011	0·079	57·8	0·093
				S 12	0·160	0·016	0·144	112·2	0·087	0·147	0·016	0·131	100·2	0·089	0·138	0·016	0·122	93·4	0·088
	4·5	0·35	−0·105	L 12	0·120	0·011	0·109	69·4	0·107	0·109	0·011	0·098	62·1	0·107	0·101	0·011	0·090	57·8	0·106
				S 12	0·186	0·016	0·170	112·2	0·103	0·166	0·016	0·150	100·2	0·102	0·159	0·016	0·143	93·4	0·103
H. With dorsal fins (props. on)	−0·5	0	−0·108	L 12	0·125	0·011	0·113	69·4	0·110	0·118	0·011	0·107	62·1	0·117	0·107	0·011	0·096	57·8	0·113
				S 12	0·179	0·016	0·163	112·2	0·099	0·162	0·016	0·146	100·2	0·099	0·164	0·016	0·148	93·4	0·108
	2·0	0·18	−0·100	L 12	—	—	—	—	—	0·102	0·011	0·091	62·1	0·100	0·098	0·011	0·087	57·8	0·103
				S 12	0·180	0·016	0·164	112·2	0·100	0·161	0·016	0·145	100·2	0·099	0·149	0·016	0·133	93·4	0·097
	4·5	0·35	−0·113	L 12	0·131	0·011	0·120	69·4	0·118	0·118	0·011	0·107	62·1	0·117	0·111	0·011	0·100	57·8	0·118
				S 12	0·192	0·016	0·176	112·2	0·107	0·173	0·016	0·157	100·2	0·107	0·168	0·016	0·152	93·4	0·111
J. With dorsal fins (props. off)	−0·5	0	−0·111	L 12	0·134	0·011	0·123	69·4	0·119	0·131	0·011	0·120	62·1	0·130	0·115	0·011	0·104	57·8	0·121
				S 12	0·193	0·016	0·177	112·2	0·106	0·165	0·016	0·149	100·2	0·100	0·165	0·016	0·149	93·4	0·109
	2·0	0·18	−0·102	L 12	0·117	0·011	0·106	69·4	0·103	0·106	0·011	0·095	62·1	0·103	0·105	0·011	0·094	57·8	0·110
				S 12	0·177	0·016	0·161	112·2	0·097	0·162	0·016	0·146	100·2	0·098	0·154	0·016	0·138	93·4	0·100
	4·5	0·35	−0·113	L 12	0·131	0·011	0·120	69·4	0·117	0·124	0·011	0·113	62·1	0·123	0·117	0·011	0·106	57·8	0·124
				S 12	0·188	0·016	0·172	112·2	0·103	0·172	0·016	0·156	100·2	0·105	0·163	0·016	0·147	93·4	0·106
L. With rope round front of fuselage (props. on)	−0·5	0	−0·087	L 12	0·104	0·011	0·093	69·4	0·091	—	—	—	—	—	—	—	—	—	—
				S 12	0·153	0·016	0·137	112·2	0·083	—	—	—	—	—	—	—	—	—	—
	2·0	0·18	−0·098	L 12	0·113	0·011	0·102	69·4	0·100	—	—	—	—	—	—	—	—	—	—
				S 12	0·175	0·016	0·159	112·2	0·097	—	—	—	—	—	—	—	—	—	—

TABLE 8

Summary of Results of the 'free runs' Giving Amplitude of Oscillation for Various Conditions of Model Tested

Tunnel Speed = 100 ft/sec

Condition of model	Angle of incidence of model, deg	Maximum half-amplitude, deg
1. Standard Case B	—0·4 2·0 4·5	±0·75 ±1·0 ±0·1
2. Transition wires on fin, Case D	—0·4	±0·75
3. Propellers fitted, Case F ..	—0·4 2·0 4·5	±0·5 ±0·75 ±0·1
4. · Dorsal fins (propellers on), Case H	—0·4 2·0	±0·5 ±0·2
5. Strakes on top of fuselage, Case K	—0·4 2·0	±0·5 ±0·25
6. Strakes on side of fuselage, Case K	—0·4	±1·0
7. Rope round fuselage in front of cockpit, Case L	—0·4 2·0	±0·5 ±0·1

20

TABLE 9

Effect of Solid Friction on the Results for the Meteor

α deg	Case	U ft/sec	Drag lb	T sec	a	Corrected n_r	Original n_r	B in. (Equation 20)	F lb-ft
− 0·4	(a) L.6	28·9	0·24	4·60	0·066 0·048	0·086	0·100	0 0·25	0 0·023
	(b) L.12	69·4	1·4	2·27	0·102 0·101	0·089	0·084	0·05 0	0·017 0
	(c) L.18	93·1	2·5	1·53	0·137 0·121	0·085	0·092	0 0·1	0 0·067
	(d) S.18	150·4	6·6	0·99	0·174 0·168	0·070	0·088	0·1 0·1	0·167 0·161
4·5	(e) L.6	28·9	0·24	4·60	0·061 0·061	0·073	0·082	0·05 0·05	0·0057 0·0057
	(f) L.12	69·4	1·4	2·29	0·108 0·102	0·091	0·095	0·025 0·025	0·0102 0·0095
	(g) S.12	93·4	2·5	1·48	0·143 0·143	0·092	0·091	0 0	0 0
	(h) S.18	150·4	6·6	1·00	0·232 0·220	0·094	0·085	0 0	0 0

TABLE 10

Effect of Drag Force on Friction (Aircraft ' A ')

Drag Force lb	$T = 2\cdot56$ sec			$T = 1\cdot74$ sec			$T = 1\cdot12$ sec			$T = 0\cdot80$ sec		
	a_f	B in.	F lb-ft	a_f	B in.	F lb-ft	a_f	B in.	F lb-ft	a_f	B in.	F lb-ft
0	0·0033	0·60	0·0080	0·0080	0·16	0·0079	0·0112	0	0	0·0125	0	0
7	0·0038	0·60	0·0092	0·0056	0·55	0·0194	0·0065	0·25	0·0164	0·0125	0	0
12	0·0041	0·55	0·0092	0·0058	0·56	0·0201	0·0080	0·10	0·0082	0·0176	0	0
17	0·0047	0·50	0·0090	0·0061	0·63	0·0241	0·0084	0·085	0·0075	0·0192	0	0
22	0·0050	0·50	0·0102	0·0054	1·05	0·0356	0·0091	0·103	0·0086	0·0155	0·08	0·021
27	0·0042	0·90	0·0155	0·0067	0·68	0·0284	0·0064	0·43	0·0246	0·0175	0·07	0·029
37	0·0039	1·10	0·0155	—	—	—	0·0047	0·0715	0·0347	0·0180	0·09	0·027

21
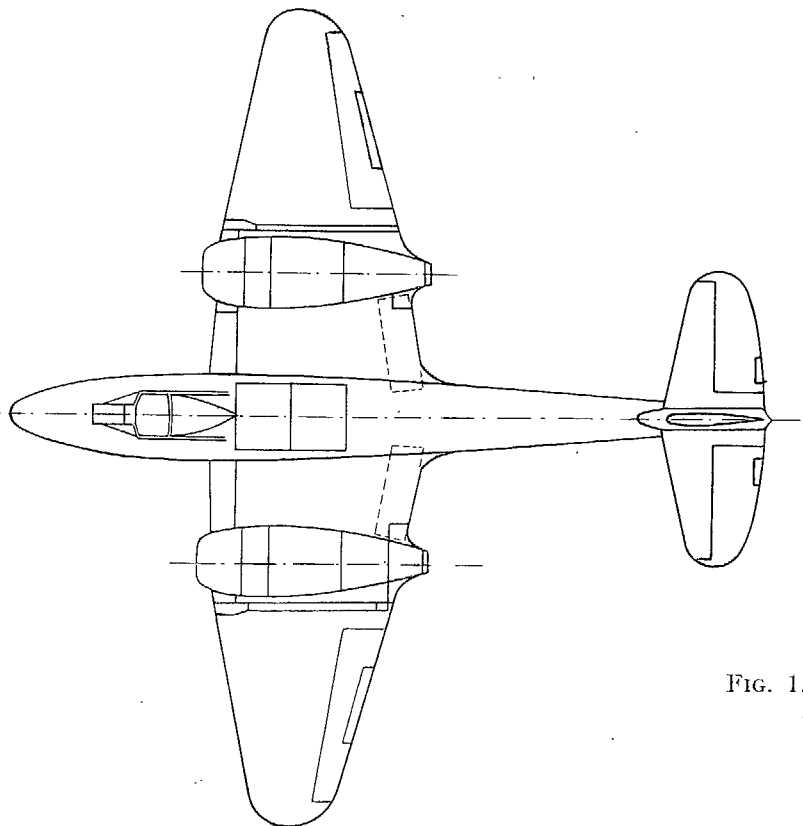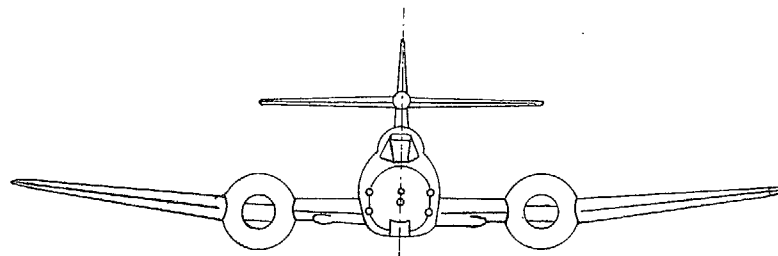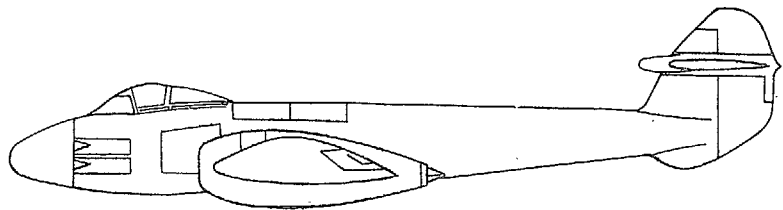
Fig. 1. General arrangement of *Meteor* MK. FIII. Standard case tested.

WOODEN FAIRING

BRACING WIRE

TURNTABLE

PEN ARM

SUPPORT TUBE

RECORDING DRUM

SPRING ADJUSTERS

CONTROL SPRINGS

SPRING LEVER ARM

AIR LUBRICATED BEARING
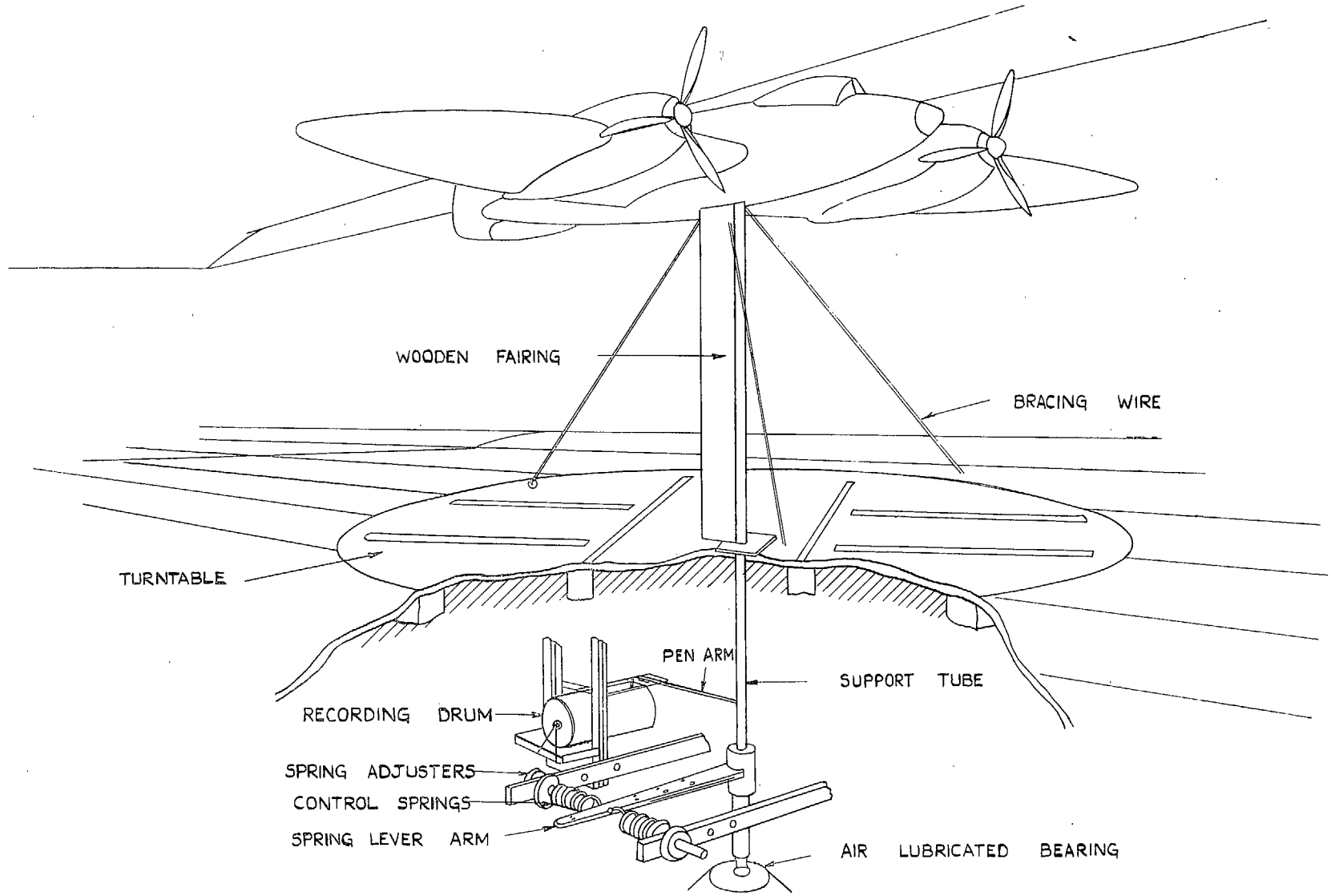
FIG. 2. Sketch showing general arrangement of model rig in wind-tunnel.

MODEL SUPPORTING-BRACKET (WITH ADJUSTMENT FOR INCIDENCE)

UPPER BALL RACE

STEEL SUPPORT TUBE A

OUTER SUPPORT TUBE B

RECORDER PEN ACTUATING ROD C

WOODEN FAIRING

BASE PLATE

TUNNEL FLOORING

TURNTABLE JOISTS

LOWER BALL RACE

RESTORING SPRING ARM

PEN ARM

HEIGHT ADJUSTMENT SCREW

AIR BEARING

AIR BEARING SUPPORT

24

NOT TO SCALE
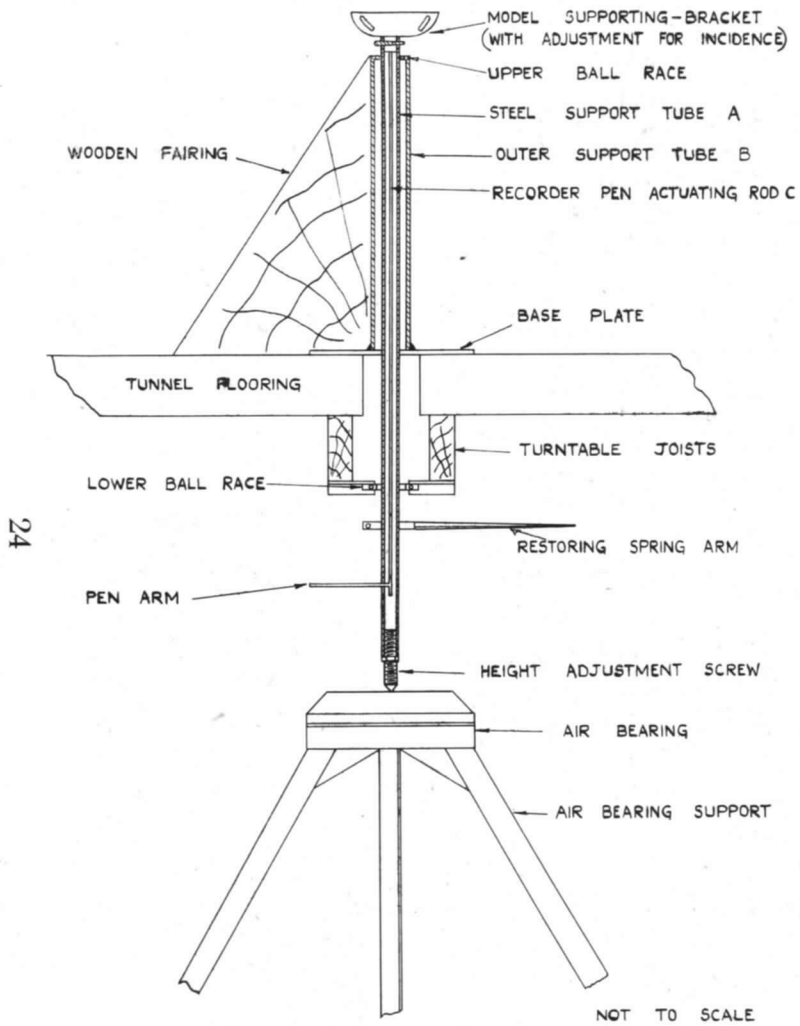
FIG. 3. Details of supporting rig for model.

LOWER BALL RACE

FIXED PLATES

SPRING TENSIONER

SPRING

SPRING LEVER ARM

RECORDING DRUM

SUPPORT TUBE A

AIR BEARING

TRIPOD
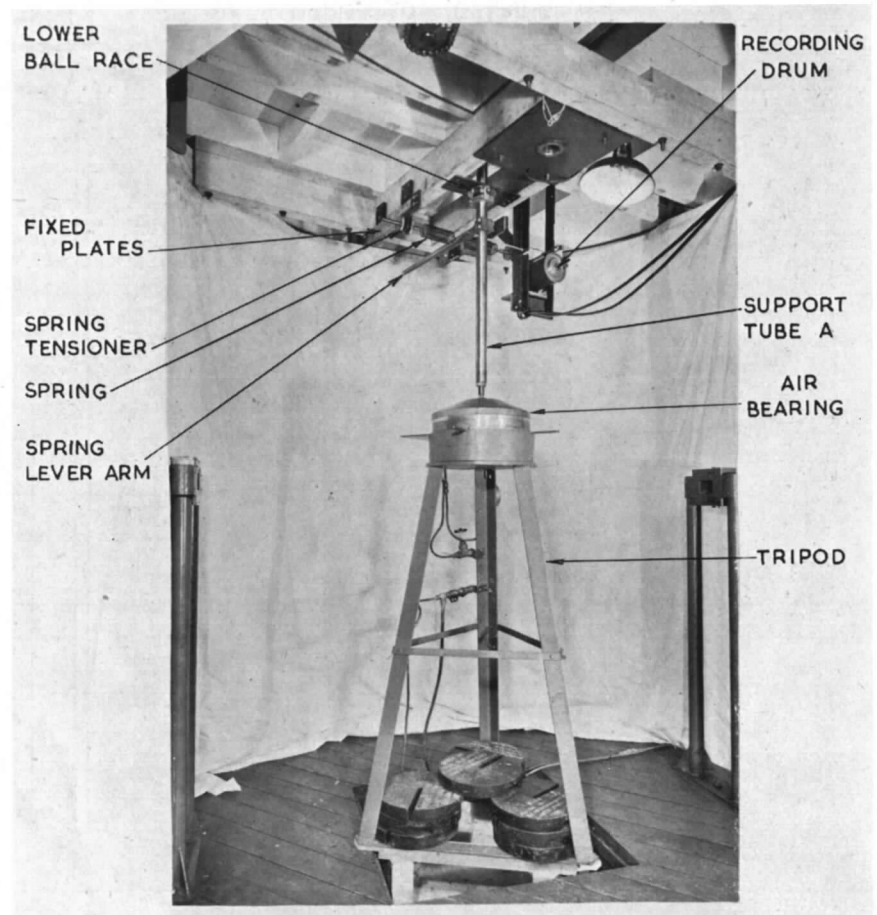
FIG. 4. Lower part of supporting rig beneath tunnel working-section.
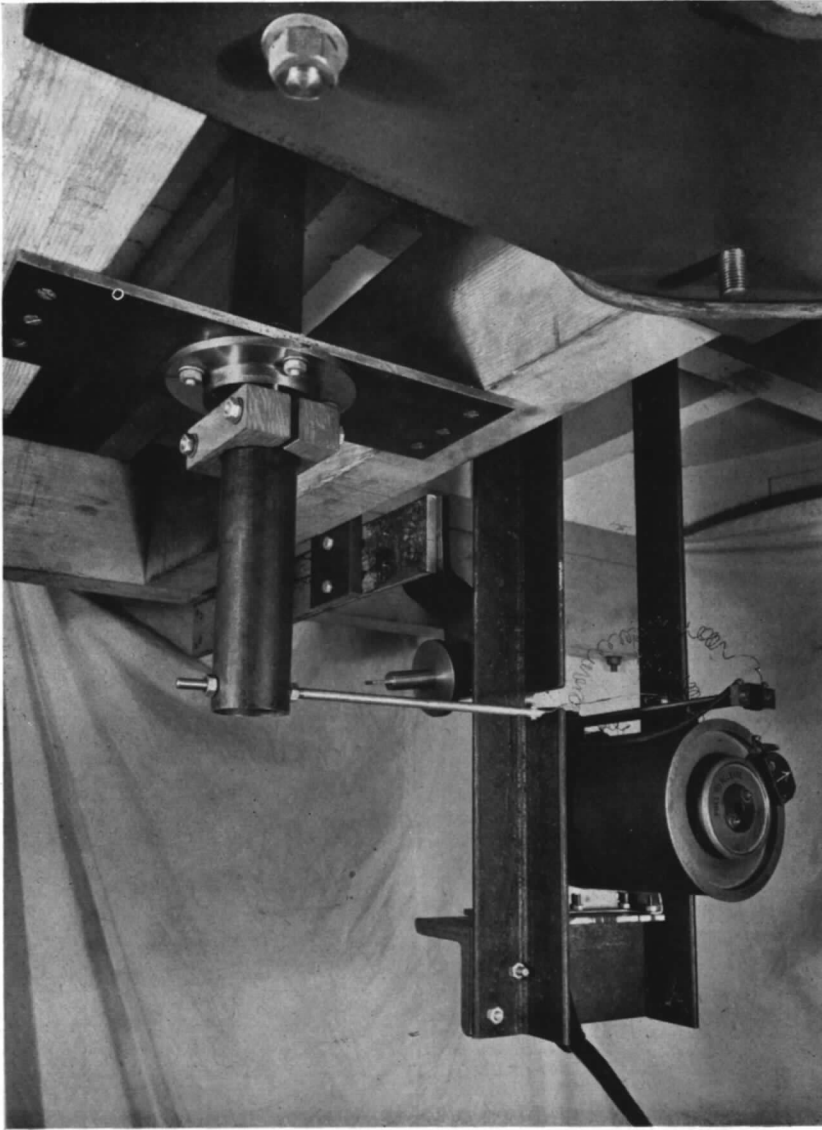
FIG. 5.   Arrangement of recording gear.   (Air-bearing removed.)
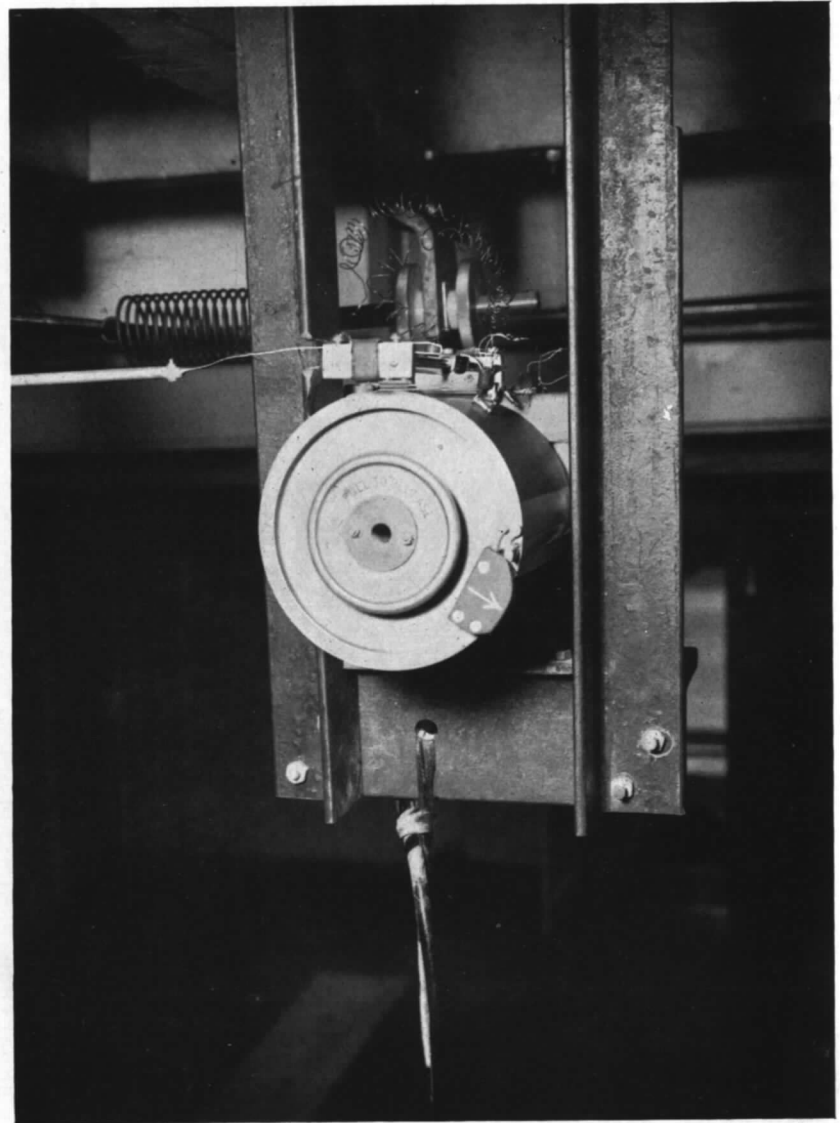
FIG. 6.   Close-up view of recording drum.
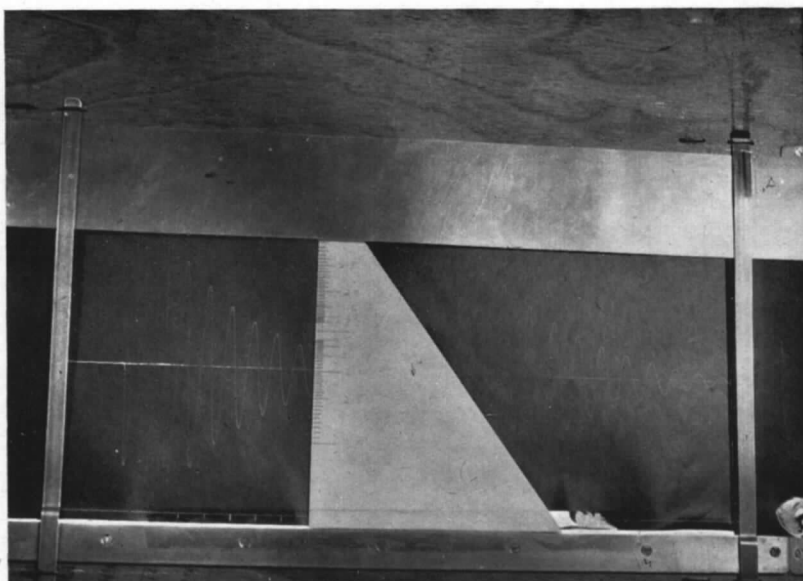
FIG. 7. Light-box showing record in position.
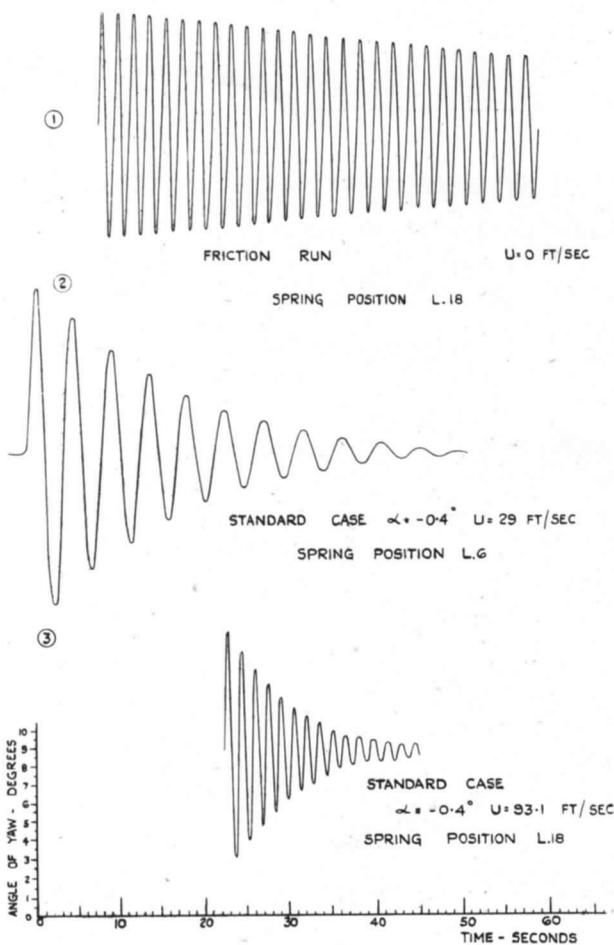
FIG. 8. Typical records of n_r runs.
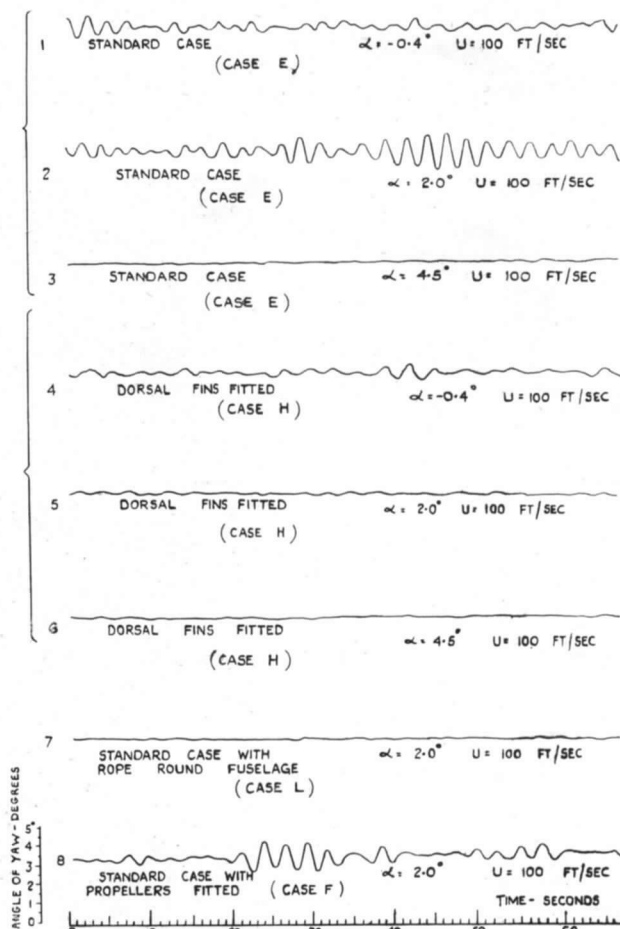
FIG. 9. Typical ' free run ' records for various conditions of model.

26
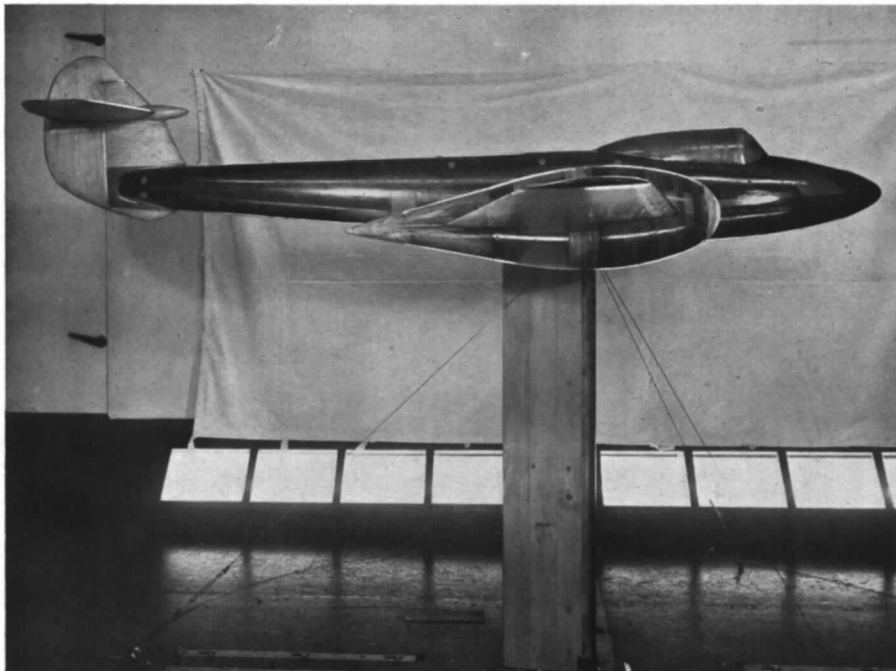
FIG. 10. Case B. Side view of standard model with nacelles blocked and faired.
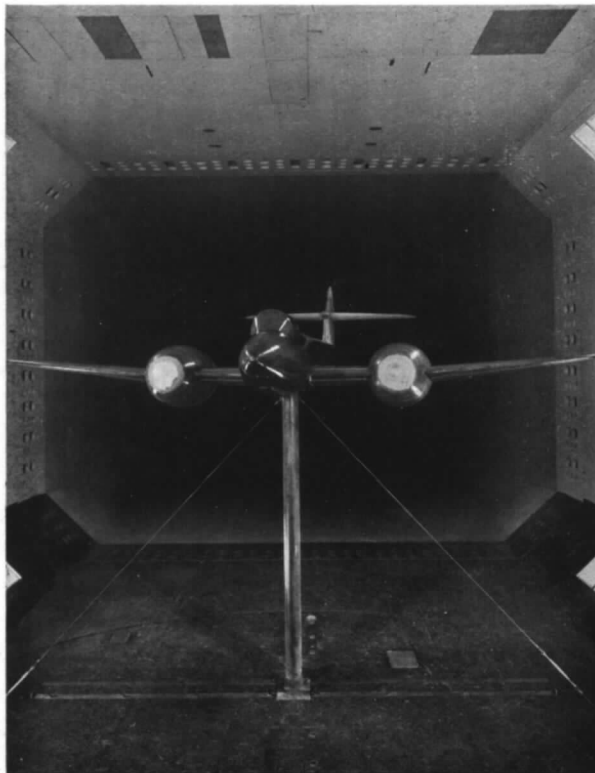
FIG. 11. Case B. Front view of standard model with nacelles
blocked and faired.

27
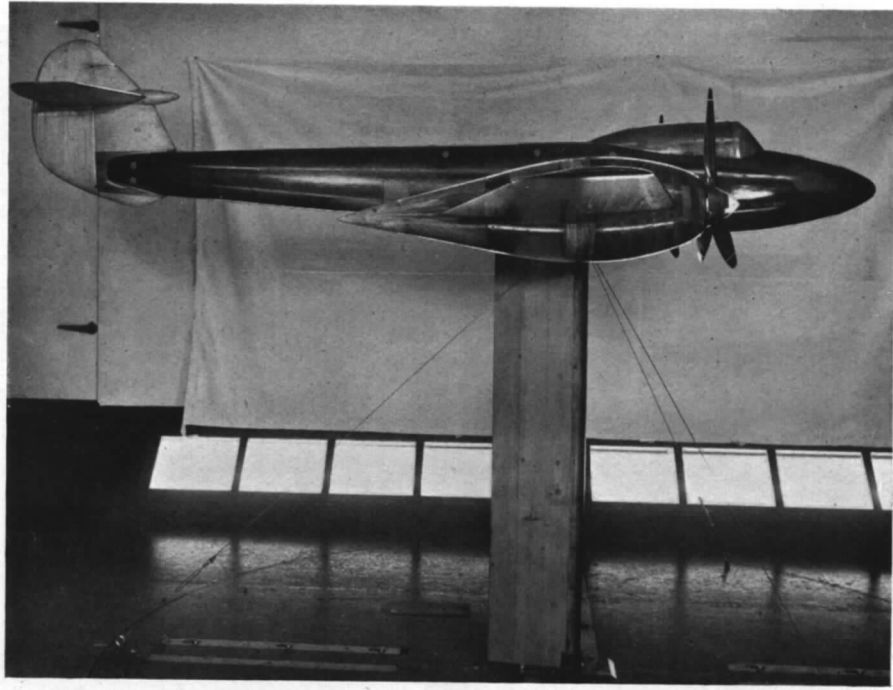
FIG. 12. Case F. Side view of model fitted
with propellers and faired nacelles.
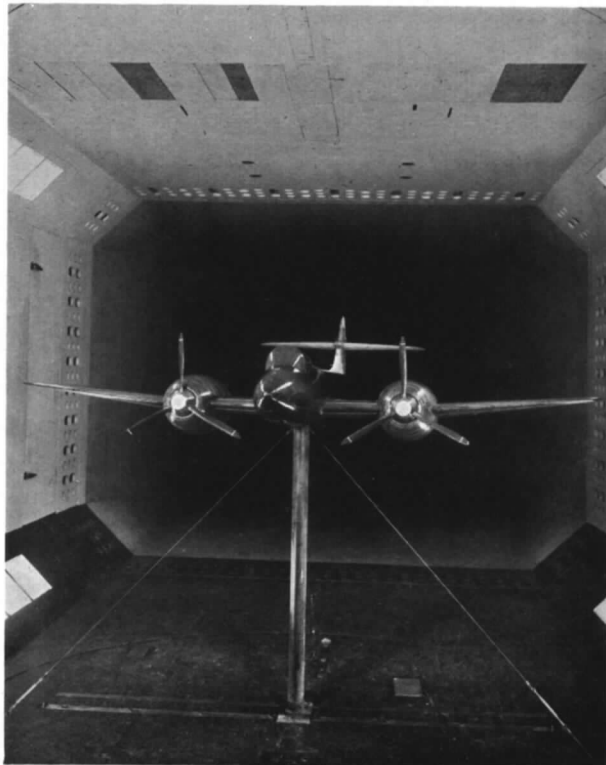
FIG. 13. Case F. Front view of model, fitted with propellers and faired nacelles.
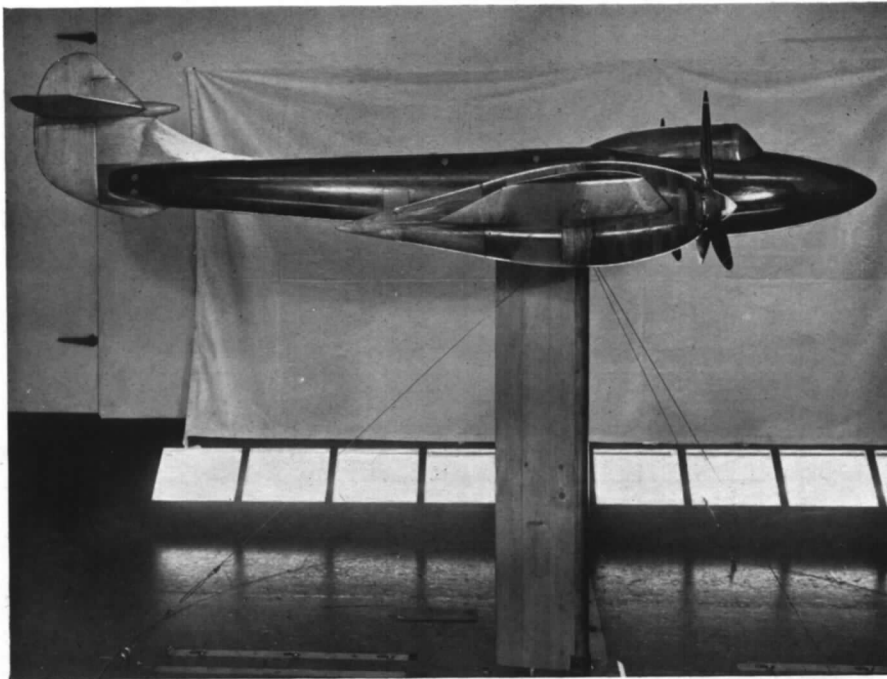
FIG. 14.   Case G.   Side view of model, fitted with propellers, faired nacelles
and upper dorsal fin.
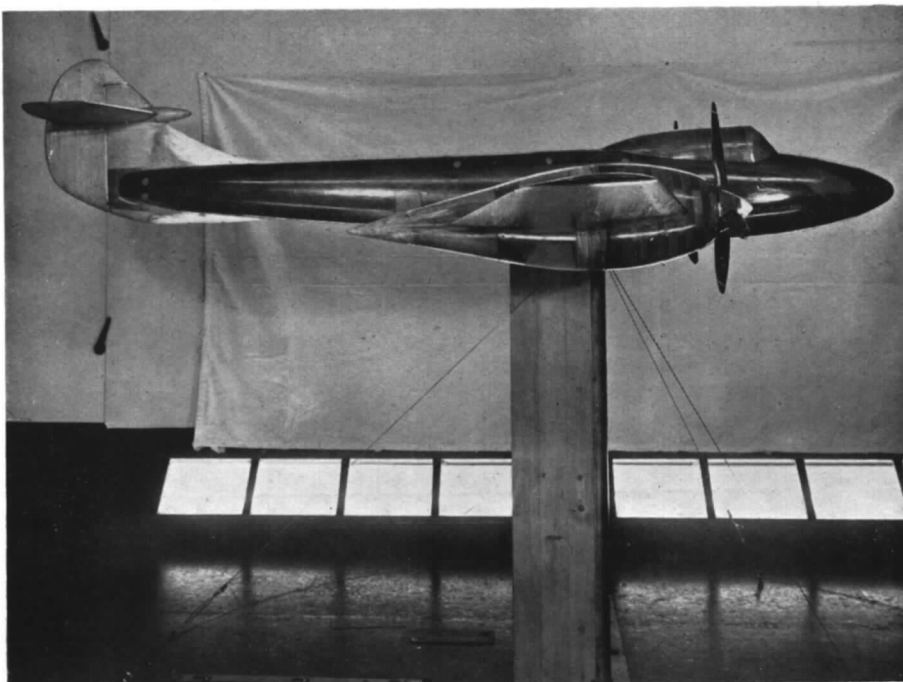
FIG. 15.   Case H.   Side view of model, fitted with propellers, faired nacelles
and with upper and lower dorsal fins.

29
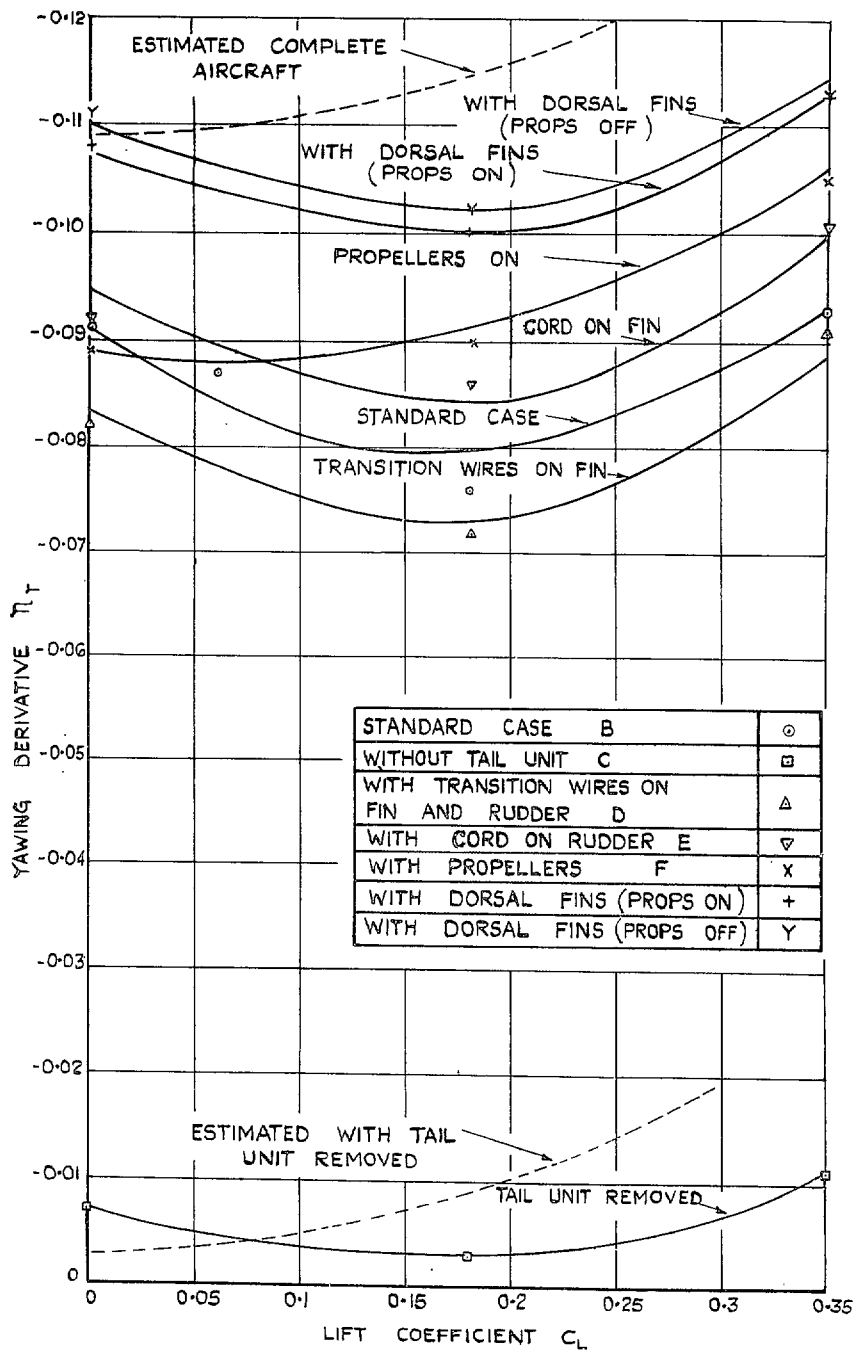
FIG. 16. Variation of lateral stability derivative n_r with lift coefficient for various conditions of model.
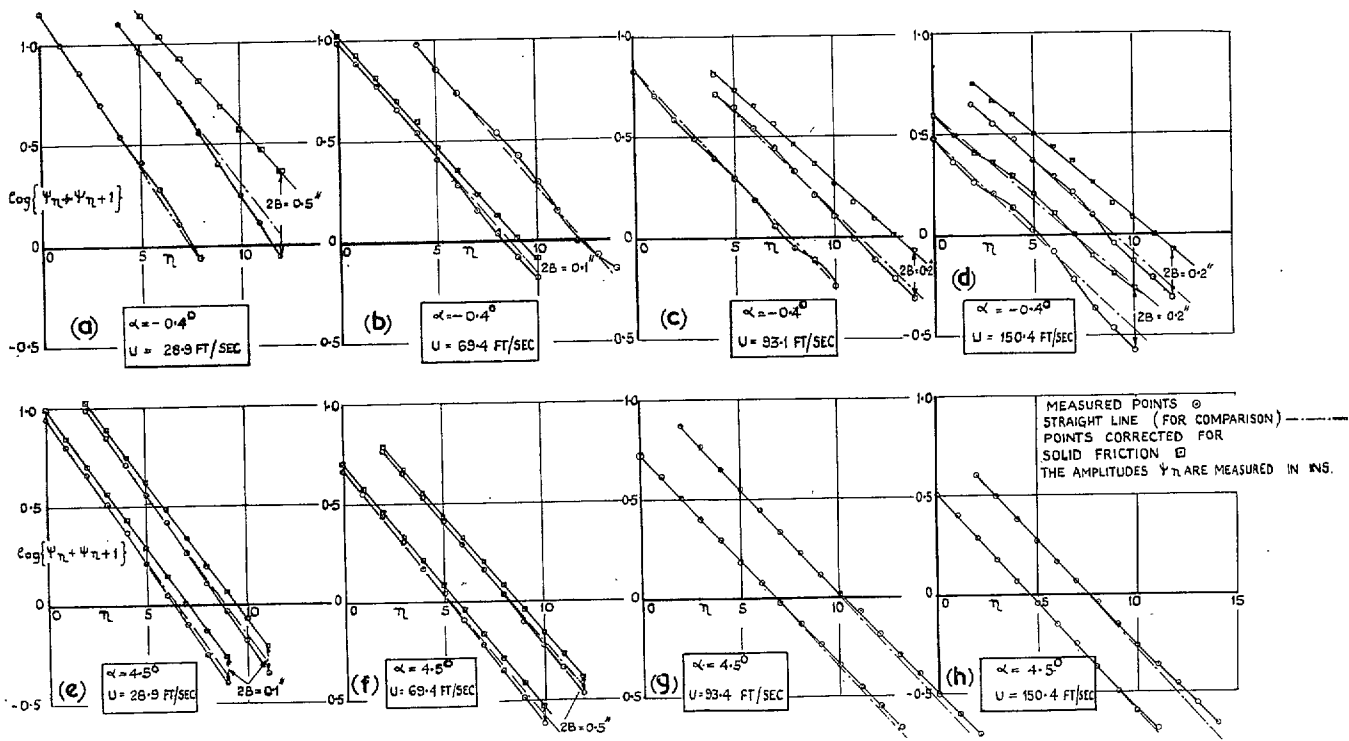
FIG. 17.   Effect of solid friction on results.

(a)   SOLID   FRICTION

(b)   DAMPING   FRICTION
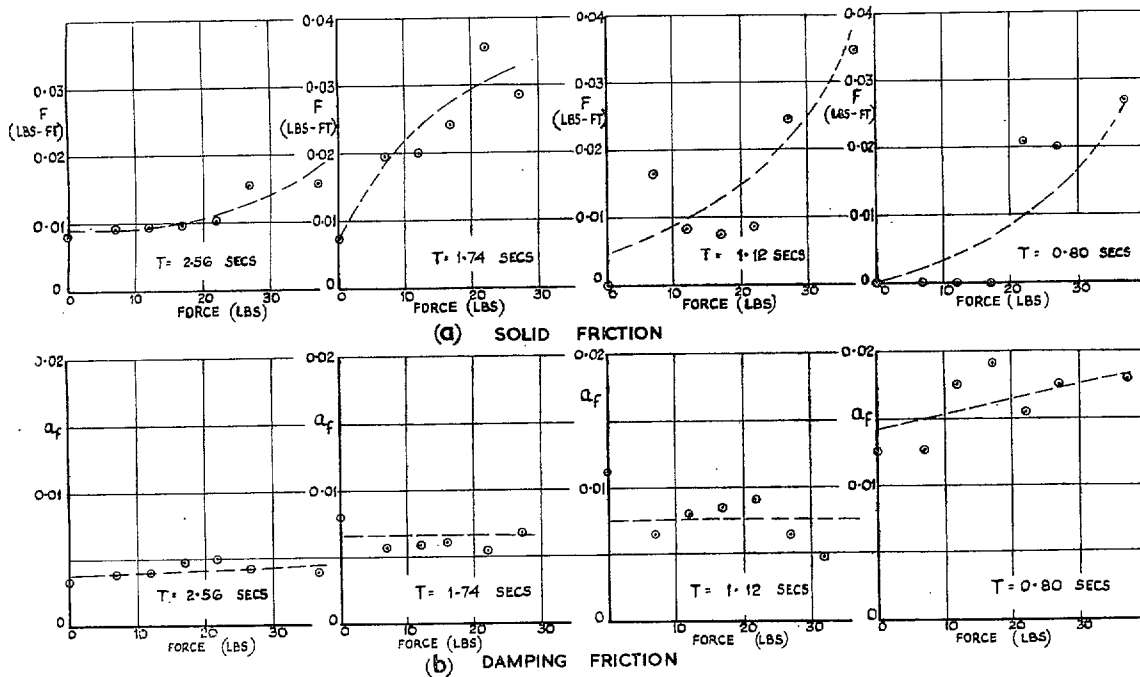
FIG. 18a and b.   Effect of Drag force on friction.

Publications of the
Aeronautical Research Council

ANNUAL TECHNICAL REPORTS OF THE AERONAUTICAL RESEARCH COUNCIL (BOUND VOLUMES)—

1934-35 Vol. I. Aerodynamics. *Out of print.*
Vol. II. Seaplanes, Structures, Engines, Materials, etc. 40s. (40s. 8d.)

1935-36 Vol. I. Aerodynamics. 30s. (30s. 7d.)
Vol. II. Structures, Flutter, Engines, Seaplanes, etc. 30s. (30s. 7d.)

1936 Vol. I. Aerodynamics General, Performance, Airscrews, Flutter and Spinning. 40s. (40s. 9d.)
Vol. II. Stability and Control, Structures, Seaplanes, Engines, etc. 50s. (50s. 10d.)

1937 Vol. I. Aerodynamics General, Performance, Airscrews, Flutter and Spinning. 40s. (40s. 10d.)
Vol. II. Stability and Control, Structures, Seaplanes, Engines, etc. 60s. (61s.)

1938 Vol. I. Aerodynamics General, Performance, Airscrews. 50s. (51s.)
Vol. II. Stability and Control, Flutter, Structures, Seaplanes, Wind Tunnels, Materials. 30s. (30s. 9d.)

1939 Vol. I. Aerodynamics General, Performance, Airscrews, Engines. 50s. (50s. 11d.)
Vol. II. Stability and Control, Flutter and Vibration, Instruments, Structures, Seaplanes, etc. 63s. (64s. 2d.)

1940 Aero and Hydrodynamics, Aerofoils, Airscrews, Engines, Flutter, Icing, Stability and Control, Structures, and a miscellaneous section. 50s. (51s.)

Certain other reports proper to the 1940 volume will subsequently be included in a separate volume.

ANNUAL REPORTS OF THE AERONAUTICAL RESEARCH COUNCIL—

1933-34	1s. 6d. (1s. 8d.)
1934-35	1s. 6d. (1s. 8d.)
April 1, 1935 to December 31, 1936.	4s. (4s. 4d.)
1937	2s. (2s. 2d.)
1938	1s. 6d. (1s. 8d.)
1939-48	3s. (3s. 2d.)

INDEX TO ALL REPORTS AND MEMORANDA PUBLISHED IN THE ANNUAL TECHNICAL REPORTS, AND SEPARATELY—

April, 1950   R. & M. No. 2600.   2s. 6d. (2s. 7½d.)

INDEXES TO THE TECHNICAL REPORTS OF THE AERONAUTICAL RESEARCH COUNCIL—

December 1, 1936 — June 30, 1939.	R. & M. No. 1850.	1s. 3d. (1s. 4½d.)
July 1, 1939 — June 30, 1945.	R. & M. No. 1950.	1s. (1s. 1½d.)
July 1, 1945 — June 30, 1946.	R. & M. No. 2050.	1s. (1s. 1½d.)
July 1, 1946 — December 31, 1946.	R. & M. No. 2150.	1s. 3d. (1s. 4½d.)
January 1, 1947 — June 30, 1947.	R. & M. No. 2250.	1s. 3d. (1s. 4½d.)

Prices in brackets include postage.

Obtainable from

HER MAJESTY'S STATIONERY OFFICE

York House, Kingsway, LONDON, W.C.2   423 Oxford Street, LONDON, W.1
P.O. Box 569, LONDON, S.E.1
13a Castle Street, EDINBURGH, 2   1 St. Andrew's Crescent, CARDIFF
39 King Street, MANCHESTER, 2   Tower Lane, BRISTOL, 1
2 Edmund Street, BIRMINGHAM, 3   80 Chichester Street, BELFAST

or through any bookseller.